Alma Mater Studiorum_Università di Bologna

Facoltà di Agraria

---

DOTTORATO DI RICERCA IN PATOLOGIA VEGETALE

SETTORE SCIENTIFICO DISCIPLINARE: AGR/12

SETTORE CONCORSUALE: 07/D1

XXIV ciclo

# Antimicrobial activity of peach and grapevine defensins

Nanni Valentina

Coordinatore:

Prof. Paolo Bertolini

Relatore:

Dott.ssa Elena Baraldi

Esame Finale anno 2012

# 1 INTRODUCTION

## 1.1 Plant innate immunity

All living organisms are continuously exposed to potential pathogens but the disease is the exception rather than the rule. The multicellular organisms are able to defend themselves against pathogen attack through the evolution of an immune system that is composed by two different systems: the innate immunity and the adaptive one. **Innate immunity** acts as the first line of defense against pathogen attack and, having an ancient origin, it is conserved among plant and animal kingdom. The **adaptive immunity**, also known as specific or acquired immunity, has evolved more recently. It exhibits a high specificity and is able to respond more vigorously to repeated exposure to the same pathogen (immunological memory). The main tools of this immune system are the antibodies.

Plants, lacking the adaptive immune system, have developed an efficient array of preformed and inducible defenses to detect and block pathogen invasions. Constitutive defenses include the presence of preformed surface wax, cell wall, antimicrobial enzymes and secondary metabolites. During the evolution, pathogens have developed strategies to overcome preformed plant defenses but plants gained the ability to organize a sophisticated set of physical and chemical inducible defense mechanisms. These are activated by two distinct classes of pathogen elicitors: general (PAMPs) and specific elicitors (encoded by the avirulence genes of a given pathogen race). A simple but elegant view of plant pathogens interaction has been shown by Jones and Dangl (Jones JD and Dangl JL, 2006) in the zig zag model (Figure 1.1).

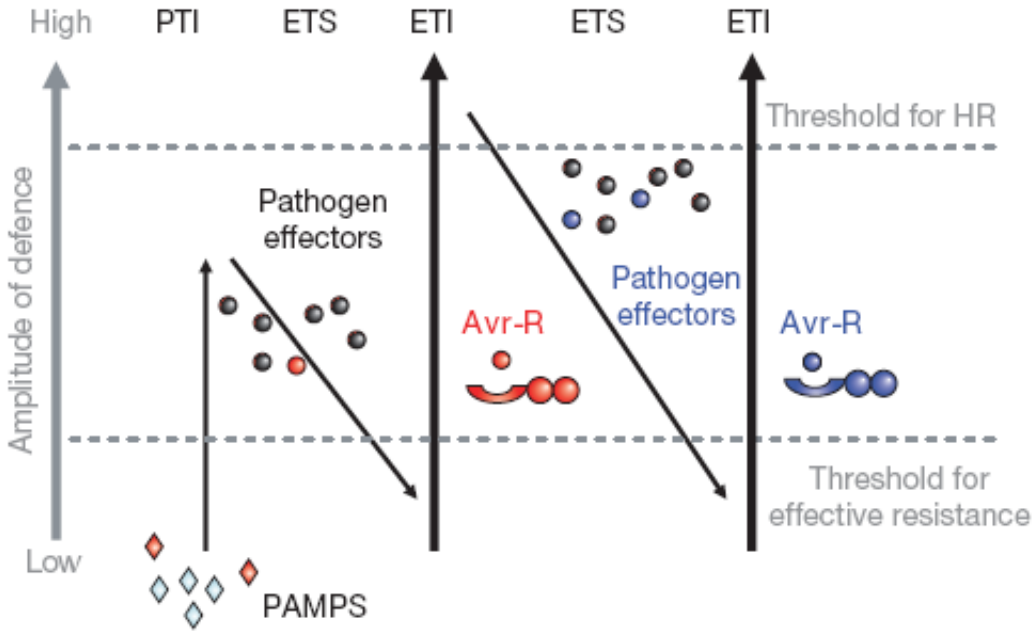


**Figure1.1 Zig zag model**. In phase 1 PAMPs or MAMPs (pathogen or microbial associated molecular pattern) are recognized by PRRs (pattern recognition receptors), resulting in PAMP-triggered immunity (PTI) that can stop further colonization. In phase 2, successful pathogens deploy effectors that contribute to pathogen virulence. Effectors can interfere with PTI and generate a effector-triggered susceptibility (ETS). In phase 3, a given effector is specifically recognized resulting in effector-triggered immunity (ETI). ETI is an amplified PTI response, resulting in disease resistance and usually in a hypersensitive cell death response (HR) at the infection site. In phase 4, natural selection drives pathogens to avoid ETI by shedding or diversifying the recognized effector gene or by acquiring additional effectors that suppress ETI.

It is commonly accepted that PAMPs induce **non host resistance** by PRRs-mediated recognition whereas specific elicitors, able to overcome the PTI, induce a **host resistance** after recognition of the product of plant resistance genes (R genes). PTI (or non-host resistance) and ETI (or host resistance), induced by general and specific elicitors respectively, constitute two forms of innate immunity in plants.


**Figure 1.2 Innate immunity of plants and animals**. The plant innate immunity (non host and host resistance) is compared to animal innate and adaptive immunity respectively (Iriti and Faoro 2007).

The plant defense responses, induced upon recognition of general or specific elicitors, are both physical and chemical, such as the deposition of callose (papilla) , the induction of hypersensitive response (HR) and **antimicrobial proteins (AMPs)** production.

Antimicrobial proteins interfere with growth, differentiation, replication or diffusion of microorganisms. Furthermore, they share common biochemical features such as small dimension (5-10 KDa), high positive charge and high number of cysteines (4-6-8-10) in their primary sequences. During the last two decades many AMPs have been isolated in plants: NCBI database (http://www.ncbi.nlm.nih.gov) reports about 1500 proteins identifiable as plant antimicrobial peptides. A classification of AMPs is shown in PhytAMP database (Hammami R *et al*. 2009), the first database completely dedicated to plant antimicrobial peptides (Figure 1.3). Among these, the most studied antimicrobial peptide families are plant defensins, thionins, lipid transfer proteins, heveine-type proteins and snakins.

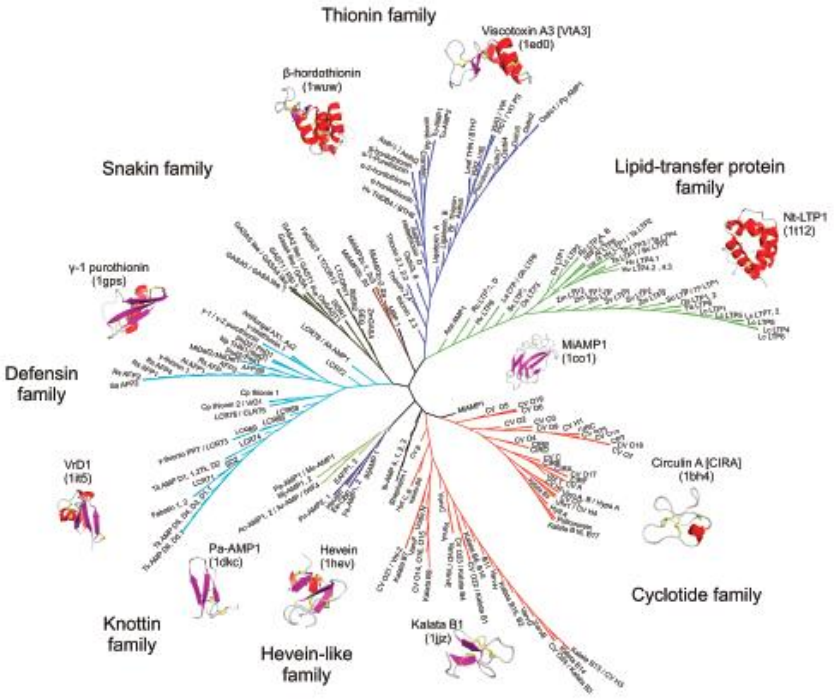


**Figure 1.3 Phylogenetic tree of plant AMPs**. A multiple sequence alignment of 271 plant AMPs was used to produce a phylogenetic tree (Hammami R *et al*. 2009) .

## 1.2 Plant defensins

Plant defensins are structurally and functionally related to defense peptides identified in several eukaryotic organisms, including mammals, birds, mollusks, insects and fungi. Phylogenetical analyses suggest that these peptides have a common ancestor and share common evolution steps. The presence of a defensin peptide in the myxobacteria *Anaeromyxobacter dehalogenans* supports the idea that they represent an ancient strategy of defense in prokaryotic life form, transferred to the eukaryotic lineage during the evolution (Carvalho AO and Gomes VM, 2009).

Plant defensins are small (about 5-6 KDa), generally basic and cysteine-rich proteins. Typically the classical number of cysteine residues is eight but defensins with 10 cysteines have been identified in tobacco and petunia.

First members of this family were isolated from the endosperm of barley and wheat and they were originally called γ-thionins for their similar size and the same number of cysteines (Mendez E *et al*. 1990). The name "plant defensins" was coined later, when the identification of two new antifungal proteins from *Raphanus sativus* (Rs-AFP1 and Rs-AFP2) permitted to notice that these proteins were more related to insect and mammal defensins than to the plant thionins (Terras FR *et al*. 1995). After that, many other plant defensins have been identified as purified proteins or deduced from cDNA, about 371 plant defensins have been so far characterized and reported in the literature (Carvalho AO and Gomes VM, 2009), considering these molecules ubiquitous among plant kingdom.

Plant defensins have been originally described as small multigene family as demonstrated by the identification of 15 genes encoding plant defensins in *Arabidospis thaliana* genome. Further studies revealed that the defensin family was fairly larger, about 300 DEFensin-*L*ike (*DEFL*) genes have been identified in *A. thaliana* (Silverstein KA *et al*. 2005)

Defensin gene structure is characterized by two exons interrupted by one intron of variable size. The first exon almost entirely encodes for the signal peptide and the second one encodes for the typical cysteine-rich domain. The signal peptide at the N-terminus is a typical hallmark for plant defensins and is considered necessary for their extracellular localization. However, recently, the plant defensin AhPDF1.1 from *A. thaliana* has been identified into the intracellular compartment, indicating possible different targeting functions for this peptide (Oomen RJFJ *et al.* 2011).

Several studies indicated that the expression of *DEFL* genes is highly variable. In normal physiologically conditions defensins have been found to be specifically expressed in plant tissue or developmentally regulated. *DEFL* transcripts are commonly abundant in reproductive tissues, such as flower, fruit and seed and, for different species, they can be found also in leaf, root and bark tissues (Terras FRG *et al.* 1995, Wisniewski ME *et al.* 2003, Fossdal CG *et al.* 2003). The constitutive expression of plant *DEFL* is consistent with a role in first-line defense of vulnerable tissues. Furthermore, the expression of several plant *DEFLs* is reported to be induced upon biotic and abiotic stress such as toxic level of salt (An SH *et al.* 2008) and zinc (Mirouze M *et al.* 2006), or fungal infection and wounding (Meyer B *et al.* 1996, Penninckx IAMA *et al.* 1996). For examples Terras and co-workers showed the gene expression of two defensins (RS-AFP3 and Rs-AFP4) in leaves of *R. sativus* upon *Alternaria brassicola* infection (Terras *et al.* 2005). A systemic transcript accumulation of *PDF*1.2, a defensin from *A. thaliana*, has been reported in arabidopsis plants infected by *A. brassicola*, involving ethylene and jasmonate pathways (Manners JM *et al*. 1998). It is commonly accepted that plant hormones as ethylene, salicylic acid, jasmonate acid and its analogue methyl jasmonate are variously implicated in signal transduction pathways that lead to the production of antimicrobial proteins.

Despite the low percentage of similarity in the primary sequence, plant DEFLs share conserved cysteine residues engaged in disulphide bridges stabilizing their tertiary structure. Plant DEFLs form a characteristic motif known as cysteine stabilized αβ motif (CS αβ) (Cornet B *et al.* 1995) and recognizable in the primary structure as **C…CXXXC…C…CXC..**

Another motif conserved among disulphide-containing antimicrobial peptides and in plant DEFL structure is **GXC($X_{3-9}$)C** (Yount NY *et al.* 2004)**.** This one, named γ-core motif, is structured in two antiparallel β strands with an interposed loop.

Three dimensional structure of some plant defensins has been resolved by NMR spectroscopy and the global fold, as typified by Rs-AFP1 (Fant F *et al*. 1998) (Figure 1.4), is an α-elix and a triple stranded antiparallel β-sheet stabilized by three intra-molecular disulphide bridges.

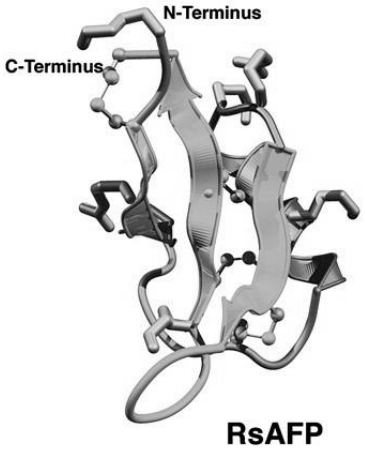


**Figure 1.4 Three-dimensional structure of the plant defensin Rs-AFP1** (Fant F *et al*. 1998)**.** In the figure the Cys side chains are represented in ball and sticks.

A wide range of biological activities has been associated to plant defensins, among these the ability to inhibit digestive enzymes such as α-amilases and serine proteinases. This function is related to plant protection role against insects. Other defensins are capable to inhibit protein translation and act as ion channel blockers. However, the most investigated activity of plant defensins is the growth inhibition of microorganisms. Plant defensins are mainly active against fungi and only few defensin peptides are known for their antibacterial function. For example VaD1, a defensin from Azuki bean, is able to inhibit *Xanthomonas campestris* and *Staphylococcus epidermidis* with IC50 of 40.8 and 36.6 μg/ml respectively (Chen CH *et al*. 2005). Interestingly, the majority of animal defensins are mainly known for their antibacterial activity.

Low concentrations of plant defensins show growth inhibition of a large spectrum of fungal species including *Aspargillus niger*, *Neurospora crassa*, *A. brassicola*, *A. solani*, *Botrytis cinerea*, *Fusarium oxysporum*, *Peniciullium expansum* and *Fusarium solani*. Furthermore, microscopical analyses revealed that some defensins are able to cause hyphae hyperbranching and swelling, classifying them as morphogenic defensins. HcAFP1, 2, 3 and 4, the four defensins recently identified from African Brassicacea species, show different level of hyper-branching morphology in *F. solani* (Figure 1.5) **(**de Beer **A** and Vivier MA, 2011**)**.

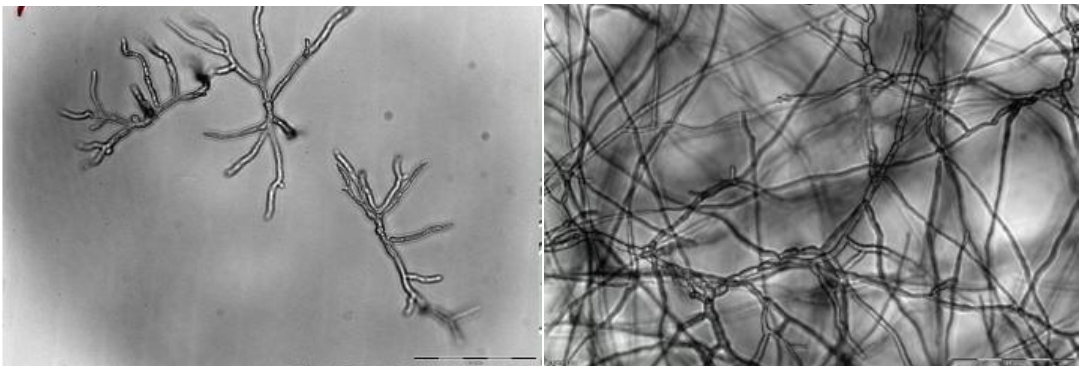

**Figure 1.5 Effect of morphogenic defensin on fungal growth**. Light microscope pictures of *F.solani* hyphae treated with the peptide Hc-AFP1 (on the left) and untreated (on the right). (de Beer **A** and Vivier MA, 2011)

An important feature shared by plant defensins (and in general by cationic antimicrobial peptides) is the electrostatic interaction between positive charges of the protein and the negative residues typically present in the outer layer of the microbial membrane. This is supported by the reduced antimicrobial activity of several plant defensins when the ionic strength of the fungal growth assay medium is increased. For examples MsDef1 (a defensin from *Medicago truncatula*), that strongly inhibits the growth of *Fusarium graminearum in vitro,* shows a reduced antifungal action in presence of $Ca^{2+}$ (Spelbrink RG *et al*. 2004). With increasing peptide concentration, the peptide molecules insert into the bilayer and lead to the distruption of membrane barrier function by different mechanisms: (i) the "barrel-stave model", which involves the formation of a permanent pore by the oligomerization of amphipathic peptide, in order to form a hydrophilic channel, (ii) the "toroidal pores model", in which the pore includes lipid head groups to stabilize the high positive charge of the peptides and (iii) the "carpet model", where layering of positively charged proteins on the plasma membranes causes destabilization in a detergent-like manner (Brogden KA *et al.* 2005).

The ability of plant defensins to induce membrane permeabilization has been widely shown by *in vitro* test against different fungi treated with SYTOX green, a fluorescent dye able to enter into the cells only in presence of compromised plasma membranes.

Research on the antifungal mode of action of plant defensins pointed already more than a decade ago to their interaction with specific binding sites in fungal membranes. Using the radiolabeled plant defensins DmAMP1 and HsAFP1, isolated from *Dahlia merckii* and *Heuchera sanguinea,* respectively, specific binding of these defensins on fungal cells and on microsomal membranes was demonstrated (Thevissen K *et al*. 1997; Thevissen K *et al*. 2000). Later, the identity of the DmAMP1 receptor on yeast membranes

was uncovered as specific inositolphosphoryl-containing sphingolipids. Also the receptor for RsAFP2, a plant defensin from radish, was identified on fungal and yeast membranes as another class of sphingolipids, namely glucosylceramide (Thevissen K *et al*. 2003). Apart from being an important structural component of eukaryotic membranes, sphingolipids are also recognized as secondary messenger molecules regulating the equilibrium between cell death and cell growth processes (Thevissen K *et al*. 2006). The structural differences between fungal/yeast and human sphingolipids could be responsible for the preferential interaction of plant defensins with fungal/yeast membranes compared to plant or human ones, explaining their low toxicity (Thevissen K *et al.* 2006).

Recently, new data have shown that membrane damage is only one among several mechanisms involved in the antibiotic action of defensins (Aerts *et al*., 2008). After the initial interaction between plant defensins and fungal membranes, several processes have been reported: RsAFP2 shows antimicrobial activity against the human pathogen *Candida albicans* through the induction of endogenous reactive oxygen species (ROS) (Aerts AM *et al*. 2007) whereas MsDef1 induces L-type $Ca^{2+}$ channel blocking in mammalian cells (Spelbrink RG *et al*. 2004), suggesting that this mechanism can possibly regulate MsDef1 antimicrobial action also against fungal pathogens. Psd1, a defensin from pea, inhibits *Neurospora crassa* fungal growth by affecting the normal progression of the cell cycle after cell internalization and interaction with fungal cyclin F (Lobo DS *et al.* 2007).

Site-specific mutagenesis studies investigated on the importance of the amino acid composition and the charge distribution of solvent-exposed loops for the antimicrobial activity of plant defensins. *In vitro* antifungal studies of mutated forms of MsDef 1 and MsDef 4 (another defensin from *M. truncatula*), using *F. graminearum* as fungal target, show that there is a positive correlation between the positive charges content of defensins and their antifungal activity. However, also hydrophobicity is crucial for defensin action, since its increase could compensate net positive charge decrease (Sagaram US *et al.* 2011). To gain a better molecular insight in the interaction between plant defensins and their sphingolipids receptors, the backbone dynamics of Psd1 and Sd5, a defensin from sugarcane, were probed and their interaction with membrane vescicles added with GlcCer was investigated (de Medeiros LN et al. 2010; de Paula VS *et al*. 2011). Both these studies showed that specific regions of the plant defensins are responsible for their ability to interact with GlcCer, ensuring anchorage to fungal membranes. Interestingly, the dynamic properties of Sd5 are completely different from those of Psd1, demonstrating that although defensins share similar threedimensional structures, their dynamic can be extremely

diverse.

The antimicrobial activity of defensin peptides has been widely studied *in vitro*. The recombinant overexpression of some defensins *in planta* showed that these peptides play also an important defense function *in planta*. For example, constitutive expression of NmDef02 (a defensin from *Nicotiana megalosiphon,* that displays a strong antimicrobial activity *in vitro* against important plant pathogens) in tobacco and potato plants enhanced their resistance against *Phytophthora parasitica* (Portieles *et al*. 2010) (Figure 1.6). Furthermore, overexpression of wasabi (*Japanese horseradish*) defensin (WT1) in rice and potato resulted in increased resistance against *Magnaporthe grisea*, *Erwinia carotovora* and *B. cinerea* (Kanzaki *et al*. 2002).

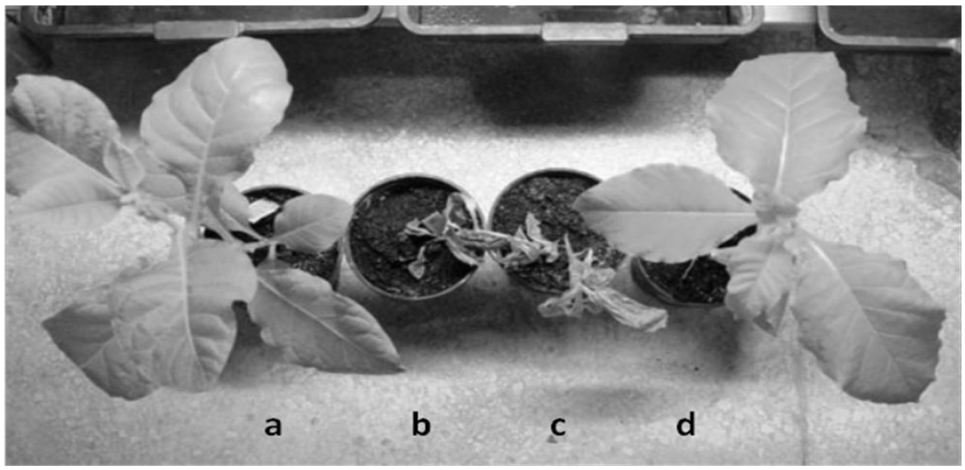


**Figure 1.6 Effect of overexpression of plant defensin *in planta***. Phenotype of tobacco plants transformed with NmDef02 (a and d) and empty vector (b and c), after *Phytophthora parasitica* inoculation (Portieles *et al*. 2010).

*In vitro* and *in planta* antimicrobial activities of plant defensins make these peptides attractive for biotechnological applications: they represent good candidates (1) for developing transgenic plants with increased resistance to pathogens and (2) for productin of natural antimicrobial peptides:

(1) Transgenic plants have the potential to provide broad resistance against different pathogens and reduce dependence on chemical pesticides. As reported above, several plant defensins have been successfully transformed into tobacco, potato and other plant species. However, at the moment, especially in European countries, the introduction of transgenic plants into agriculture has been vigorously opposed, mainly for the risk to mix transgenic and non transgenic crops and for the possibility of endangering native or non target species.

(2) The study of natural antimicrobial peptides as alternative to chemical pesticides or in general as drugs is currently under investigation. The increased use in the last decades of antibiotics in biomedical and agriculture fields has led to the emergency of more resistant and virulent strains of pathogens and the urgent need for highly effective antimicrobials. The use of antimicrobial peptides (AMPs) is a promising approach for several interesting characteristics: they feature (a) broad-spectrum antimicrobial activity against fungi, bacteria and virus, (b) small dimension (c) high protein stability (d) low IC50 values, (e) synergism with other AMPs, (f) low toxicity against mammal cells and (g) as part of the non-host resistance, pathogens will not develop resistance. The reduced toxicity towards animals could be explained by the dependence of membrane interaction caused by AMPs to lipid composition of the target membrane; it's known that there are differences between plant, animal and yeast/fungal membrane composition (Wilmes *et al*. 2011).

Plant defensins have all positive characteristics here reported, however, production of recombinant defensins is difficult and expensive. Until now, the cost associated with defensin production has represented the major obstacle for the widespread use of these peptides as antimicrobial agents. The recombinant expression of plant defensins in *Escherichia coli* or *Pichia pastoris* is commonly performed for *in vitro* antimicrobial activity test, but with these systems the final protein yield is generally low, representing a obvious problem for the mass production.

# 2 PROJECT AIM

Before this study, only one defensin in peach, PpDFN1 (Wisniewski ME *et al.* 2003), and one in grapevine, VvAMP1 (de Beer A and Vivier MA 2008), were known. Moreover, there were no data available regarding the antifungal activity of PpDFN1. The main objective of this work was the characterization of the antimicrobial activity and the mode of action of PpDFN1 and identify and study novel DEFL (DEFensin Like) peptides from grapevine.

A prerequisite for these objectives was the development of a suitable protocol for their production and for this reason a consistent part of this PhD work was invested in developing protocols suitable for the recombinant expression and purification of peach and grapevine DEFLs. Several studies reported the difficulties to produce reasonable yields of these small peptides in heterologous expression systems. Production of DEFLs with a quick, easy and cheap protocol is considered a preliminary step in order to study antifungal properties and for a possible future exploitation as antimicrobial peptides in different fields.

The antimicrobial activity of peach and grapevine DEFLs was investigated using different techniques, such as fluorescence microscopy, monolayer technique and mutagenesis studies. Understanding mechanism of action involved in the susceptibility of fungi to DEFLs may provide new insight into the inhibitory activity of these antimicrobial peptides and lead the development of new antifungal compounds in agriculture.

The biological role of **PpDFN1** in peach has been analyzed by studing the *Ppdfn1* gene expression in flower, fruit and leaf and its induction in fruits upon *Monilia laxa* (the main fungal pathogen infecting *Prunus spp.*) infection.

In order to characterize the PpDFN1 activity, the peptide was overexpressed in *Escherichia coli* as recombinant protein and purified to homogeneity through chromatographic techniques. The purified recombinant PpDFN1 was tested against fungal and bacterial pathogens and its mechanism of action was investigated using different strategies. The PpDFN1 ability to permeabilize the membranes of sensitive fungi was

analyzed by fluorescence microscopy and its interaction with lipids investigated using monolayer techniques. The affinity of PpDFN1 for different lipids was studied using monolayers composed of lipids of different origin.

In the laboratory of Dr. Moser at FEM-IASMA (Trento, Italy), 79 sequences encoding for **DEFL** peptides were identified in **grapevine** (Giacomelli L *et al.* paper submitted), by scanning the *V. vinifera* sequenced genome (Velasco R *et al.* 2007). The identified sequences were included in four groups depending on their cysteine pattern, and candidates from each group, displaying a different gene expression pattern, were selected for the recombinant expression in *E. coli*. The purified recombinant peptides (DEFL 13, 22 (VvAMP1), 31 and 59) were tested *in vitro* for their antimicrobial activity against *Botrytis cinerea*; DEFL 13, showing the strongest antifungal potency, was selected for investigation on the mechanism of action, using different techniques. Among these, a *B. cinerea* mutant library, depleted in genes encoding for signal transduction proteins, was screened in order to identify possible pathways involved in DEFL 13 antifungal action. In addition, site-direct mutagenesis of DEFL 13 was performed to identify key residues important for protein activity.

During the PhD, I have had the possibility to work for six months in the laboratory of Dr. Mark Banfield (Biochemestry Laboratory. John Innes Centre, Norwich. UK). During this experience I optimized the cloning, the expression and the protein purification of grapevine DEFLs, which allows me to familiarize with the protein chromatography AKTA system (GE Healthcare). I also worked for two months in the laboratory of Prof. Paul Tudzynsky (Biology and Biotechnology of fungi. University of Muenster, Germany), where I had the possibility to screen the DEFL 13 action against a collection of *B. cinerea* signaling mutants. Both these experiences represented fundamental steps of my PhD, considering the results obtained further to my personal and professional formation.

# 3 MATHERIALS AND METHODS

## 3.1 Gene expression, antimicrobial activity and membrane interaction of the peach (*Prunus persica*) defensin PpDFN1

### *3.1.1* BLAST search of peach *DEFLs*

To identify DEFL encoding genes, the peach (*Prunus persica*) genome predicted peptide V 1.0 (http://www.rosaceae.org) database was scored by BLAST search using PpDFN1 as query. Retrieved peptide sequences were aligned using CLUSTAL X software (Larkin MA *et al.* 2007) and the percentages of identity and similarity were calculated using EMBOSS software (Rice P *et al.* 2000).

### 3.1.2 RT-qPCR analysis of *Ppdfn1* gene expression

Leaves, flowers and fruits (at different ripening stages: S1- enlargement of pericarp; S2- pit hardening; S3- enlargement of the mesocarp; S4- climacteric phase) of the peach (*Prunus persica*) cv K2 were harvested from a local fungicide-free orchard (Bologna-Italy). The whole leaves and flowers and the peel of the fruits were immediately frozen in liquid nitrogen. S3-stage fruits were inoculated with a conidial suspension of *Monilia laxa* at a concentration of about $10^6$ conidia/ml. Three replicates of 15 fruits each were dipped for 1 min in the fungal conidia suspension or in water for the control. The peach fruits were then conserved at 20°C for 24 and 48 h and the peel samples were immediately frozen in liquid nitrogen. Total RNA was isolated from each tissues (leaf-flower-S1,S2,S3,S4-fruits and S3 *M. Laxa* and mock inoculated fruits), following the protocol published by Bonghi *et al*. (Bonghi C *et al*. 1992) with some modifications. Briefly, 0.2 g of frozen tissues were ground to a fine powder in liquid nitrogen with mortar and pestle and the ground tissue was suspended in 800 µl of 65°C preheated extraction buffer and leaved at 65°C for 10 min. One volume of 65°C preheated phenol was added to the mixture and samples were centrifuged at 14000 g for 6 min. The upper phase was extracted with en equal volume of

phenol:chloroform:isoamylalchol (25:24:1), re-centrifuged and re-extracted with one volume of chloroform:isoamylalchol (24:1). After centrifugation at 14000 g for 6 min, the RNA was precipitated in one volume of isopropyl-alcohol and 0.3 M sodium acetate (pH 4.8), washed with 70% ethanol and resuspended in TBE (Tris/Borate/EDTA). RNA was then precipitated in 3M LiCl overnight at 4°C, centrifuged at 30000 g for 30 min and washed with 70% ethanol. The pellet was resuspended in 30 µl of DEPC (DiethylenePyrocarbonate)-treated water. DNA was removed from the samples by Turbo DNase treatment (Ambion) following the manufacturer's instructions. RNA purity was analyzed by measuring the A260:A230 and A260:A280 ratios and the quantity was calculated from the adsorbance at 260 nm. In order to analyse the integrity of the samples 0.5 µg of RNA was run on agarose gel (Figure 2.1).

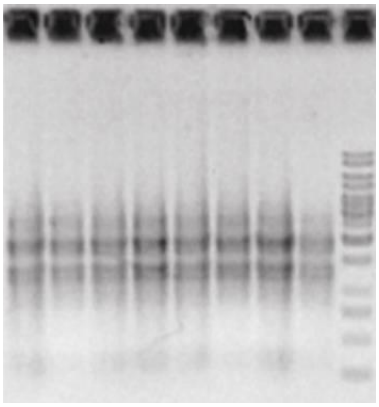

**Figure 3.1. Agarose gel of total RNA samples**. The integrity of RNA was indicated by the presence of the two ribosomal RNA bands. In the last lane the 1kb Gene Ruler (Fermentas) was loaded.

The first strand cDNA was synthesized from 500 ng of total RNA using the ImProm-II Reverse TranscriptaseTM kit (Promega), following the manufacturer's instructions. Suitable primers for Real Time PCR were designed to specifically amplify *Ppdfn1* and *actin* (as normalizer) genes using the software Primer3 (http://frodo.wi.mit.edu/primer3/-primer3code.html). Primer sequences were as following

***Ppdfn1****:* Forward primer 5'CGCTCCATGCGTTTATTTTC

Reverse primer 5'TCACAGGTCCTAGCCTCAGC

***Actin***: Forward primer 5'ATCATGTTTGAGACCTTCAATG

Reverse primer 5'AGAGTCCAGCACAATACCAGTT

The primers were synthesized by PRIMM srl.

Real Time PCR was performed on MX3000 machine (Stratagene) using the Brillant

SYBR Green qPCR Master mix (Stratagene). Three biological replicates for each sample and two technical replicates of each reaction were always run in the same experiment. All thermal cycles started with an initial denaturation step at 95°C for 10 min, followed by 40 cycles consisting of a denaturation step at 95°C for 30 sec, an annealing step at a specific temperature (60°C for the *Ppdfn1* and 58°C for *actin*) and an extension step at 72°C for 1 min. Quantification was carried out using the standard curve generated by serial dilutions of a cDNA first strand randomly chosen. Data were analyzed using MXPro QPCR Software, Version 3.0 (Stratagene).

### 3.1.3 Cloning, expression and purification of PpDFN1

The cDNA encoding for PpDFN1 mature peptide was amplified from total cDNA generated from fruit at the S2 ripening stage. Specific oligonucleotides were designed and the restriction enzyme recognition sites (BspHI in the forward and HindIII in the reverse primer) were introduced to insert the gene in the multi-cloning site of pHAT (Peranen J *et al*. 1996) and pET32 (Novagen). Both the vectors are selected for the ability to produce a N-terminal His-tagged protein; pET 32 is designed for also adding a thioredoxin (TRX) as N-terminal fusion protein.

**Forward primer** 5' TATATCATGAGGACCTGTGAGTCTCAGAGTAAT

**Reverse primer** 5' TATAAAGCTTTTAACAATGTTTAGTGCAAAAGC

The restrictions sites introduced are underlined. The primers were synthesized by PRIMM srl.

The PCR was performed with 25 pmol of each primer, 2 mM dNTP mix, 1.5 mM $MgCl_2$, 1x buffer and 1 U of GoTaq polymerase (Promega). PCR started with an initial denaturation step at 95°C for 5 min, followed by 35 cycles (95°C for 1 min, 60°C for 45 sec and 72°C for 45 sec) and a final extension at 72°C for 5 min. PCR amplification was analyzed on agarose gel and purified with Nucleospin Extract II kit (Macherey-Nagel) following the manufacturer's instructions. The total amount of purified PCR product was digested with 25 U of each restriction enzyme (Fermentas) at 37°C for 3 h. The digested PCR product was gel-purified (Nucleospin Extract II kit Macherey-Nagel), eluted in sterile water and quantified on agarose gel. 60 ng of purified PCR product was ligated with 18 ng of digested (with the NcoI and HindIII digestion enzymes) pHAT or pET32 vectors by 2 U of T4 ligase (NEB) and incubated at 16°C overnight. The recombinant plasmids were introduced in *E. coli* DH5α strain by electroporation and transformed cells were grown

overnight at 37°C in Luria-Bertani solid media. For plasmid selection, ampicillin (100 μg/ml) was added to all media. Liquid cultures were prepared from a single colony and the cells were grown in LB media with agitation. Plasmids were purified using the Nucleospin Plasmid kit (Macherey-Nagel).

DNA fragments cloned into the plasmids were sequenced by BMR-genomics (www.bmr-genomics.it) using the universal T7 forward primer (5'TAATACGACTCACTATAGGG-3'). The chromatograms were analyzed with Chromas software available on the BMR-genomics website.

The recombinant vectors were introduced in *E. coli* BL21(DE3) Origami cells (Novagen) by electroporation. Origami host strain has a mutations in both the thioredoxin reductase (*trxB*) and glutathione reductase (*gor*) genes, which enanche disulphide bond formation in the cytoplasm. Bacterial cultures were grown in LB medium supplemented with ampicillin (100 μg/ml) at 37°C by shaking up to an absorbance value of about 0.5 at 600 nm. The protein expression was induced for 3 h at 37°C or overnight at 20°C by adding 0.4 mM isopropyl 1-thio-b-D-galactopyranoside (IPTG). A small scale expression test was performed and the production of recombinant protein was checked in SDS-PAGE gel, in order to select the vector and to chose the optimal expression conditions.

The pellet obtained from *E. coli* BL21 Origami transformed with recombinant pET32 and induced overnight at 20°C was resuspended in 50 mM phosphate buffer, 300 mM NaCl, 20 mM imidazole, 10% glycerol, pH 8 and lysed by French press (SLM AMINCO I) at 1200 psi. The lysate was centrifuged and the filtered (0.45 μm) supernatant applied to pre-equilibrated 5 mL $Ni^{2+}$-NTA (nickel-nitrilotriacetic agarose) columns (GE Healthcare). After a wash with a washing buffer containing 20 mM of imidazole, the protein was eluted with 200 mM imidazole. Fractions containing fusion protein (as identified by SDS-PAGE gel) were pooled, concentrated and dialyzed against digestion buffer (20 mM Tris-HCl, 50 mM NaCl, 2 mM $CaCl_2$, pH 8). TRX-6xHis tag was removed by enterokinase (Novagen) digestion (0.0001% w/w) overnight at 20°C. PpDFN1 was further purified by cationic exchange chromatography (MonoS, GE Healthcare); a NaCl gradient was performed to separate the proteins with different calculated pI.

| Protein | Molecular weight | pI | Coefficient of extinction |
|---|---|---|---|
| **TRX-6xHIS-PpDFN1** | 22409.3 | 6.40 | |
| **PpDFN1** | 5437,2 | 9,17 | 500 |
| **TRX-6xHIS** | 16990.1 | 5.33 | |
| **Enterokinase** | 26306.8 | 5.35 | |

**Table 3.1 Biochemical features reported for TRX-6xHis-PpDFN1, PpDFN1, TRX-6xHis and enterokinase**. The parameters reported in the table are calculated using the free program Protparam (http://web.expasy.org/protparam).

Fractions containing PpDFN1 were pooled, concentrated and dialyzed in phosphate buffer, 150 mM NaCl, pH 8. PpDFN1 was spectrophotometrically quantified (Spectrophotometer *ND-1000*, Nanodrop) based on absorbance at 280 nm reported in the table 3.1 and checked for purity in SDS–PAGE gel.

### 3.1.4 Antimicrobial activity of recombinant PpDFN1

For *in vitro* antifungal activity test, fungi (*Botrytis cinerea*, *Penicillium expansum* and *Monilia laxa*) were grown on potato dextrose agar (PDA, Difco). The PpDFN1 antifungal activity was assayed by evaluating inhibition of conidia germination of *M. laxa*, *B. cinerea* and *P. expansum*. Percentage of inhibition was measured by spectrophometer in a 96-wells micro-titer plate; each well contained 100 µl of water and 1% glucose, 2000 spores and 40-0 µg/ml of purified PpDFN1. Control reactions contained protein buffer without peptide. Plates were incubated at 20°C and the spetrophotometric readings were taken every 24, 48 and 72 h at 620 nm. All readings were corrected by subtracting the time zero readings. Each assay was independently repeated three times with three technical replicates per measurement. Percentage of growth inhibition was calculated as follow: % of growth inhibition = 100 x ($A_{control} - A_{sample}$) / $A_{control}$ , where A is the corrected absorbance at 620 nm of the control or the sample.

The IC50 values of PpDFN1 were calculated after 72 h of incubation.

Antibacterial activity of PpDFN1 was similarly assessed in a 96 wells micro titer plate. Wells contained 100 µl of minimum media (M9 Minimal salt, Sigma-aldrich), bacterial culture at $OD_{600}$ of 0.1 and 100 µg/ml of PpDFN1. The control reactions contained protein buffer without peptide. Plates were incubated by shaking for 48 h at 37°C and the bacterial growth was monitored by measuring the absorbance at 600 nm every 24 h. The assay was used to test antimicrobial activity against *Xanthomonas*

*campestris*, *Psedumonas auroginosa* and *Agrobacterium tumecians* and against *Listeria monocitogenes* and *Salmonella enteritidis*. The same assay was performed also for the yeast *Saccharomyces cerevisae*.

### 3.1.5 Fluorescence microscopy analysis

SYTOX green (Invitrogen) assay was performed as previously reported by Thevissen and co-workers with some modifications (Thevissen K et al. 1999). Briefly, water and 1% glucose containing *M. laxa*, *B. cinerea* or *P. expansum* (2.5 x $10^4$ conidia/ml) were incubated for 18 h at 20°C. PpDFN1 at concentration of 40 µg/ml and SYTOX green (1 µM) were added and after 6 h of incubation (at the dark) the germinated conidia were analyzed using a Dialux 20EB, Leitz microscope. Samples were excited at 504 nm and the SYTOX green fluorescence was monitored at 523 nm. Images were captured and processed using Nikon Eclipse TE2000-E program.

### 3.1.6 Monolayer measurements

The monolayer experiments were performed with a commercial apparatus (µTrough S; Kibron) enclosed in a plexiglass cabinet and connected to a computer. The surface pressure $\pi$ of the lipid monolayer is defined as the decrease in surface tension $\gamma$, i.e., $\pi=(\gamma o- \gamma m)$, where $\gamma m$ and $\gamma o$ represent the surface tension of the water/air interface in the presence or absence of the lipid monolayer. It was measured by the Wilhelmy method, using a 2 mm diameter platinum wire, which ensures a zero contact angle. Before each experiment, the trough and the wire were thoroughly cleaned with hot water and organic solvents, followed by a final wash in MilliQ water. Solutions were stirred with a thin teflon-covered magnetic bar. All measurements were made at 23°C. To minimize the amount of defensins required, the experiments were performed in a small, home-made, circular teflon trough (total surface 2.54 $cm^2$, total volume 800 µL). Defensin was injected directly into the subphase through a hole drilled in the trough wall. Before the protein was applied, a lipid monolayer was prepared adding lipids in small drops on the top of the buffer surface until the desired initial surface pressure was reached. To attain a steady state, the monolayer was allowed to stand for at least 30 min before the defensin was injected. The experiments were performed preparing the monolayer with different lipids, reported in the table 2.2.

| Abbreviation | Type of lipids | Comments |
|---|---|---|
| **P** | Total lipids of *P. Expansum* | Folch extraction* |
| **M** | Total lipids of *M. Laxa* | Folch extraction* |
| **B** | Total lipids of *B. Cinerea* | Folch extraction* |
| **ePC:cer** | egg L-α-phosphatidylcholine bovine and brain ceramide β-D-galactoside 2% | Commercial lipids (Sigma-Aldrich) |
| **ePC** | egg L-α-phosphatidylcholine | Commercial lipids (Sigma-Aldrich) |
| **RBC** | Total lipid of human erythrocyte | Folch extraction* |

**Table 3.2 Different lipids assayed in monolayer experiments**. In the table, the abbreviation, the ype of the lipids and the comments about the origin of the lipids are reported. Before use the commercial lipids were dissolved in chloroform/methanol solution (2:1 v/v) up to lipid concentration of 25 μg/ml. Red blood cells were centrifuged from freshly collected blood (from healthy volunteers) and washed three times with vesicles buffer (10 mM Hepes, 140 mM KCl and 0,1 mM EDTA pH 7.4) before the Folch extraction.

* Folch extraction (Folch J *et al*. 1957). Briefly 20 mg cells and 3 ml solution (10 mM Tris, 250 mM sucrose pH 7) were homogenized on ice using homogenizer Ultra Turrax T8 (IKA Labortechnik) and 20 mg glass beads (212-300 μm, Sigma-Aldrich) followed by centrifugation (5000 g, 20 min, 4°C). The supernatant was extracted with chloroform/methanol (2:1 v/v) and separated from the sediment by centrifugation (5000 g, 30 min, 25°C). The sediment was re-extracted with chloroform/methanol (1:2 v/v) and supernatants were combined, dried by rotary evaporation and dissolved in chloroform/methanol/distilled water (54:31:15v/v) mixture. The solution was shaken vigorously and the two phases were separated by centrifugation (600 g, 20 min, 25°C). The lower phases was re-extracted sequentially with chloroform/methanol/distilled water (37:34:29 v/v) mixture. Finally the lower phase was dried by rotary evaporation and kept at -20°C under gas nitrogen. Before using they were dissolved in chloroform/methanol solution (2:1 v/v) at 25 μg/ml.

## 3.2 Identification and characterization of the defensin-like gene family in grape (*Vitis vinifera*)

### 3.2.1 Genome identification of *DEFL* sequences and analysis of their primary structure

The identified grapevine DEFLs (Giacomelli L *et al*. paper submitted) were aligned using CLUSTAL X software (Larkin MA *et al.* 2007) and the groups were formed considering the cysteine residues pattern.

### 3.2.2 Selection of grapevine DEFLs, recombinant expression, purification and antimicrobial activity

Primers containing specific extensions (table 3.3) were used to amplify the mature form of DEFL 1, 13, 22, 31 and 59 from cDNAs.

| *DEFL* | Forward primer (5'-3') | Reverse primer (5'-3') |
|---|---|---|
| **1** | AAGTTCTGTTTCAGGGCCCGCAAGATCCAGGGAGTGATTG | ATGGTCTAGAAAGCTTTAAGCAATAATACAACAACAAC |
| **13** | AAGTTCTGTTTCAGGGCCCGCAACAAGATGGAAGGTGTTGCAA | ATGGTCTAGAAAGCTTTAACAATAACAATGACAAACATGACGA |
| **22** | TATATCATGAGGACCTGAGAGTCAGAGCCAC | TATAAAGCTTTTAACAATGCTTAGTGCAGAAGC |
| **31** | AAGTTCTGTTTCAGGGCCCGGCGGATCCACAAAAAAGTTGC | ATGGTCTAGAAAGCTTTAACAAGGGTACATGTACAC |
| **59** | AAGTTCTGTTTCAGGGCCCG AAGGAGGTTAAGGCAGCGAGG | ATGGTCTAGAAAGCTTTAACAGTTGTAATAGCAAATACATTC |

**Table 3.3 Forward and reverse primers used for the cloning in expression vectors**. For the *DEFL* 22 the restriction sites (BsphI in the forward and HindIII in the reverse primer) and the "tata" sequences are underlined. For the other *DEFLs*, appropriate In-Fusion™ extensions are underlined. The primers were synthesized by PRIMM srl.

(a) DEFL 22 (VvAMP1)

The amplification product of *DEFL* 22 was cloned into pHAT (Peranen J *et al*. 1996) and pET32 (Novagen) vectors for the recombinant expression. The cloning strategy, the protein expression and the purification protocols were the same used for PpDFN1.

(b) DEFLs 1, 13, 31 and 59

A versatile ligation-independent cloning method was pursued for *DEFL* 1, 13, 31 and 59 (Berrow *et al*. 2007). Appropriate primer extensions were used to enable In-Fusion™ cloning into the digested pOPIN F and M vectors to obtained the desired 6xHis-tagged proteins. PCRs were performed in 50 µl reaction mixes using TAQ polymerase (Invitrogen), with 30 pmol of each forward and reverse primers and either 0.5 ng of the cDNA (from inflorescence for *DEFL* 13 and 59, from seed for *DEFL* 31 and from fruit for *DEFL* 22) as template per reaction. The resulting PCR products were separated by electrophoresis on a 1% w/v agarose TBE gel and purified from the gel using the QIAquick™ kit modified for gel extraction (Qiagen). Purified PCR products were eluted from the QIAquick™ columns in 50 µl of pure water. About 100 ng of purified PCR products and 100 ng of the linearized pOPIN F or M vector were mixed in the wells of an

In-Fusion$^{TM}$ Dry-Down (Takara-Clontech) and incubated at 42°C for 30 min. All reactions were diluted 1:5 with TE Buffer (10mM Tris, 1mM EDTA pH 8.0) and 15 µl were used to transform chemical competent *E. coli* DH5α cells by heat shock method. The transformants were selected by plating on LB Agar plates supplemented with the carbecillin (100 µg/ml), 0.02% w/v X-Gal and 1mM IPTG and incubating overnight at 37°C. The positive white colonies were inoculated in LB supplemented with carbecillin. The cultures were used for plasmid preparation using the kit Wizard plus Miniprep (Promega), following the manufacturer's instructions. Plasmids were screened using the PCR protocol described above for *DEFL* amplifications except the forward primer which was replaced with the standard T7 forward primer. The PCR products were analyzed by electrophoresis on a 1 % w/v Agarose TBE gel and DNA fragments were sequenced by BMR-genomics. The chromatograms were analyzed with Chromas software available on the BMR-genomics website and positive recombinant vectors were transformed into chemical competent *E. coli* Origami strain (Novagen) by heat shock. The plates were incubated for 18 h at 37°C before individual colonies were used for small scale expression test. Bacterial cultures were grown in LB medium supplemented with carbecillin (100 µg/ml) at 37°C by shaking up to adsorbance values of about 0.4-0.5.at 600 nm. The protein expression was induced by adding 0.4 mM IPTG for 3 h at 37°C or overnight at 20°C. The recombinant expression was analyzed by SDS-PAGE gel for selecting the construct and the optimal expression conditions.

Pelleted cells from 6 l of bacterial cultures able to express the recombinant soluble protein (pOPIN M-*DEFL* 13, 31 and 59 induced overnight at 20°C) were resuspended in lysis buffer (50 mM Tris-HCl, 500 mM NaCl, 20 mM imidazole, 50 mM glycine, 20% (v/v) glycerol, pH 8) and lysed by a constant cell disruption systems (CONSTANT SYSTEMS LTD). The lysates were centrifuged at 18000 g for 30 min and the filtered (0.45 µm) supernatants were applied to pre-equilibrated 5 ml $Ni^{2+}$-IMAC columns (GE Healthcare) and proteins were eluted with 500 mM imidazole. Fractions containing fusion proteins (MBP-6xHis-DEFL 13, 31 and 59) were identified by SDS-PAGE gel, pooled and concentrated, then injected into a Hi-Load 16/60 Superdex 75 column (GE Healthcare) pre-equilibrated with 20 mM HEPES, 150 mM NaCl pH 7.5. The MBP-6xHis tag was removed by digestion with C3 protease (12 µg/mg of fusion protein) overnight at 4°C. The MBP fusion partner and the 3C protease were removed using MBP and HIS trap columns linked in series (5ml, GE Healthcare). The flow through from these columns were

concentrated and injected onto a Hi-Load 16/60 Superdex 75 column (GE Healthcare) pre-equilibrated with 20 mM HEPES, 150 mM NaCl, pH 7.5. The fractions containing protein were pooled, concentrated and their purity was confirmed by SDS-PAGE gel. Proteins were quantified by their absorbance at 280 nm (Spectrophotometer ND-1000, Nanodrop ) and the concentration was calculated using the corresponding ε (table 3.4).

| DEFLs | calculated ε | Molecular weight |
|---|---|---|
| **13** | 9105 | 6417.1 |
| **22** | 500 | 5557.3 |
| **31** | 3480 | 5554.4 |
| **59** | 4970 | 5939.8 |

**Table 3.4 Extinction factors (ε) and the molecular weights (MW) of mature DEFLs**. The parameters were calculated by Protparam (http://web.expasy.org/protparam)

The purified proteins were assayed for quantify the number of free sulfhydryl groups in solution using the Ellman's test Kit (Thermo Scientific) (Ellman GL 1958).

The *in vitro* antimicrobial activity against *B. cinerea* was assayed both by microscopical observation of spore germination and by spectrophotometric determination of the IC50 values. The *in vitro* assays were performed in 96-well micro-titer plates containing 100 µl half Potato Dextrose Broth (PDB, Difco) with 5 x $10^4$ spores/ml of *B. cinerea* and the purified DEFLs at concentration from 0 to 50 µg/ml. Plates were left at 20°C for 3 days. After 16 h, conidia germination was checked with an inverted microscope to observe some possible morphological changes. Protein buffer and buffer added with the reduced and alkylated form of each recombinant DEFL were used as controls. Reduced and alkylated forms were obtained by addition of 2 mM Tris[2-carboxyethyl] phosphine hydrochloride and incubation for 5 min at 95°C, follwed by addition of 15 mM iodoacetic acid to the cooled reaction mixtures and incubated for 30 min in the dark. The samples were dialyzed overnight at 4°C against 20 mM HEPES, 150 mM NaCl pH 7.5 and quantified.

Spectrophometric readings were taken after 24, 48 and 60 h at 540 nm and corrected for their time zero readings. Grapevine DEFLs activities were scored after 60 h and expressed in terms of % of growth inhibition, which is defined as

$100 \times (ABS540_{control} - ABS540_{sample}) / ABS540_{control})$

where $ABS540_{control}$ and $ABS540_{sample}$ are the corrected absorbance measured at 540 nm of control (buffer) and sample (DEFLs) respectively. Each activity assay was repeated three times with independent *B. cinerea* cultures.

## *3.3* Characterization of the antimicrobial activity of DEFL 13 from *Vitis Vinifera*

### 3.3.1 Optimization of recombinant DEFL 13 expression and purification

The recombinant expression of DEFL 13 in *P. pastoris* was tried following the instruction reported in "EasySelect *Pichia* Expression Kit" (Invitrogen).

Briefly, the cDNA encoding for DEFL 13, depleted of the signal peptide, was amplified from total cDNA generated from grapevine inflorescence. Specific oligonucleotides were designed for cloning the gene in the pPICZα vector (Invitrogen), EcoRI and XbaI restriction enzyme sites were added in the forward and reverse primer respectively. In the reverse primers 2 stop codons (TTATCA), 6 codons codifying for histidine (GTGATGGTGATGGTGATG) and 3C protease site (CGGGCCCTGAAACAGAACTTCCAG) were also introduced.

Forward primer (5'-3'):

GTACATgaattccaacaagatggaaggtgttgcaaag

Reverse primer (5'-3'):

CATGTAtctagaTTATCAgtgatggtgatggtgatgcgggccctgaaacagaacttccagacaataacaatgacaaacatgacgacc

The restrictions sites introduced are underlined. The primers were synthesized by PRIMM srl.

*DEFL* 13 was amplified by PCR (as reported above for grapevine *DEFLs* cloning) and cloned in the vector pPICZα at the corresponding sites. The gene follows the α factor signal for secreted expression and AOX1', the highly methanol-inducible and tightly regulated promoter (Figure 2.2).

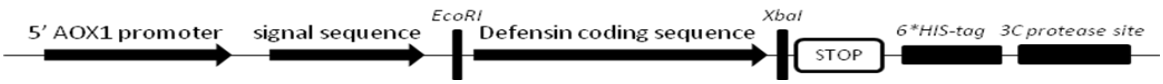


**Figure 3.2 Expression vector pPICZα-6xHis-*DEFL* 13**. The recombinant vector was constructed for the extracellular expression of DEFL 13 fused to 6xHis-tag and 3C protease recognition site at its C-terminal after two stop codons. EcoRI site in the 5' and XbaI site in the 3' were also created.

The recombinant vector was used to transform *E. coli* DH5α, colony PCR and restriction digestion by EcoRI and XbaI were carried out in order to confirm the recombinant trasformants. The positive clones obtained were verified by sequencing (www.bmr-genomics.it) using 5'AOX universal primer (5'GACTGGTTCCAATTGACAAG) and chromatograms were analyzed with Chromas software available on the BMR-genomics website. The constructed vector pPICZα-6xHis-*DEFL*13 was linearized with PmeI, purified and transformed in *P. pastoris* GS115 strain competent cells by electroporation. The cells were selected in YPDS plate (yeast extract peptone dextrose) supplemented with zeocine (100 μg/ml) and incubated at 30°C for 48 h. Ten colonies of transformed *P. pastoris* were selected for small scale expression test in shake flasks containing 5 ml of BMGY (buffered complex glycerol medium) liquid medium until the A600 value reached 2. The cultures were centrifugated at 3000 g for 5 min and the cell pellets were resuspended in 10 ml of BMMY (buffered complex methanol medium) medium (A600 value of 1). The methanol (5% v/v) was daily added for 5 days and 1 ml of sample was collected every day for SDS-PAGE analysis. The extracellular and intracellular proteins were checked by SDS-PAGE gel and stained using InVision™ His-tag In-gel Stain (Invitrogen), a fluorescent stain specifically formulated for sensitive and specific detection of His-tagged fusion proteins.

The recombinant vector pOPIN M-*DEFL* 13 was trasformed in *E. coli* SHuffle strain (NEB), a commercial engineered *E. coli* strain capable of cytoplasmatic expression of proteins rich in disulphide bridges.

Furthermore, in order to decrease the loss of protein during the last purification step (size exclusion chromatography), two alternatives were tested: (a) $Ni^{2+}$NTA (GE Healthcare) and amylose affinity chromatography (MBPtrap HP GE Healthcare) connected in series and (b) cationic exchange chromatography (SP Sepharose High Performance, GE Healthcare) both directly performed after the 3C protease cleavage. (a) The sample was loaded to pre-equilibrated affinity columns linked in series and the flow through was collected. (b) The sample was loaded to pre-equilibrated column and after washing with

the buffer A (20 mM HEPES, 150 mM NaCl pH 7.5) a linear gradient up to 100% of buffer B (20 mM HEPES, 1 M NaCl pH 7.5) was performed. The fractions corresponding to chromatogram peaks were collected and analyzed by SDS PAGE gel. Peaks containing the DEFL 13 were pooled, concentrated and their purity was confirmed by SDS PAGE.

### *3.3.2* Antimicrobial activity against fungal and bacterial pathogens

The purified DEFL 13 was assayed in vitro (following the protocol reported above for B. cinerea) against several fungal pathogens: Colletotrichum acutatum, Fusarium oxysporum, Monilia laxa, Aspargillus niger, Alternaria arboresca, Penicillium expansum and Trichoderma spp. Furthermore, the antimicrobial activity of DEFL 13 was tested against the plant pathogenic bacteria Agrobacterium tumefaciens and Erwinia amylovora in micro plate assay. Wells contained 100 µl of minimum media (M9 Minimal salt, Sigma-aldrich), bacterial culture at $OD_{600}$ of 0.1, and 100 µg/ml of DEFL 13 or protein buffer without peptide for the negative control reactions. Plates were incubated by shaking for 48 h at 30°C and the bacterial growth was monitored by measuring the absorbance at 600 nm every 24 h.

### *3.3.3* Effect of cations on the antifungal activity

The effect of the DEFL 13 on the *B. cinerea* conidia germination was tested at different concentration of protein (50, 25, 12.5, 6.25 and 3.13 µg/ml) in half PDB medium supplemented with 50 mM, 25 mM and 12.5 mM KCl and 5 mM, 2.5 mM and 1.25 mM $MgCl_2$. For each medium a negative control consistent in the same volume of protein buffer (20 mM HEPES, 150 mM NaCl pH 7.5) was performed. The antimicrobial activity of the different concentrations of protein in each medium was analyzed following the protocol reported above and the percentage of inhibition was calculated after 24 h of peptide incubation.

### *3.3.4* Thermal stability of DEFL 13

The secondary structure of DEFL 13 and thermal treated DEFL 13 was evaluated by CD spectroscopy. The protein sample (5 µM) was dissolved in 50 mM phosphate buffer, pH 7.5 using a JASCO 810 spectropolarimeter and a cuvette with 0.1 cm path length. Ten

spectra were accumulated from 190 to 240 nm at 0.2 nm intervals and averaged to achieve an appropriate signal to noise ratio. The spectrum of the buffer was substracted. The same experiment was conducted associating protein thermal denaturation (90°C for 10 min). The secondary structure composition of the peptide was evaluated using CONTIN tool available on the Dichroweb server (Withmore and Wallace, 2004) and the obtained values were used to have an estimation of the relative amount of secondary structure elements.

The thermal treated DEFL 13 was used in order to investigate the thermal stability of the peptide, evaluating the percentage of *B. cinerea* growth inhibition respect to the untreated DEFL 13. The antimicrobial activity was analyzed and the percentage of inhibition was calculated after 24 h of incubation (as reported above).

### *3.3.5* Activity against fungal hyphae and protoplast of *B. cinerea*

The ability of DEFL13 to block the fungal growth of *B. cinerea* was tested against the actively growing mycelium. 50 μg/ml of DEFL 13 or the same volume of buffer (for the negative control) were added to overnight germinated conidia (5 x $10^4$ conidia/ml of half PDB) and the morphological effect of the protein on the fungal hyphae was observed by microscope after 2 h of incubation. The spectrophotometric readings were taken at time 0, 24 and 48 h and the % of growth inhibition was calculated as reported above.

The antimicrobial activity of the DEFL 13 was assayed against the protoplast of *B. cinerea*, generated following the protocol reported by Schulze Gronover C *et al*. (Schulze Gronover C *et al*. 2001).

Briefly, a spore suspension of *B. cinerea* was inoculated in PDB and incubated for 24 h in agitation at 20°C. The filtered young mycelium was washed and incubated in agitation for 2 h at 28°C with an enzyme solution of 40 mg Novozym 234 (Novo Enzyme products Ldt.) for ml of KC solution (600 mM of KCl and 60 mM of $CaCl_2$). The protoplast solution was filtered, washed and centrifuged twice at 4000 g for 10 min at 4°C. The pelleted protoplast was resuspended in KC buffer. A solution of 5 x $10^4$ protoplasts/ml of half PDB and 50 mM glucose were used for the 96 wells plate antimicrobial activity test and the % of growth inhibition was calculated after 24 h of DEFL 13 incubation, as reported above.

### 3.3.6 Fluorescence microscopy analysis

The SYTOX green assay was performed following the instruction reported above for PpDFN1, except to the medium that changes from 1% glucose to half PDB and the time of protein incubation (from 6 h to 2 h).

DEFL 13 was labeled with fluorescein isothiocyanate (FITC) via reactive amines, through incubation in the dark for 1 h. Unlabeled FITC was removed by filtration in a Centricon YM-3 vial (Millipore). The adsorption at 494 nm was determined, and subsequently, the degree of labeling was calculated by the following equation:

dye per protein molecule = (A494 x diluition factor)/ (68000 x protein concentration),

where 68000 is the molar exctintion factor of FITC at 494 nm. The antimicrobial activity of FITC-labeled DEFL 13 was tested before fluorescence assays as reported for the other antimicrobial assays. A solution of 5 x $10^4$ conidia/ml grown for 18 h in a half PDB was treated with FITC-labeled DEFL 13 (50 μg/ml) for 1 h. The fluorescence was observed using a Dialux 20EB Leitz microscope. Samples were excited at 488 nm and FITC fluorescence was monitored at 509 nm. Images were processed using Nikon Eclipse TE2000-E software.

### 3.3.7 Screening of DEFL 13 activity on signaling mutants of *B. cinerea*

The antifungal activity of DEFL 13 was tested against a collection of knock-out *B. cinerea* mutants depleted to specific genes involved in signaling cascade. This collection (reported in Table 3.5) was created by Prof. Paul Tudzynsky and co-workers in the laboratory of Biology and Biotechnology of fungi (University of Muenster, DE) and kindly provided for this screening.

| Mutated gene | Gene function | Comment | Reference |
|---|---|---|---|
| Bc1g_14021 | Bc- and Ss-specific ??? | BotBank project | Giesbert et al., *submitted to MPMI* |
| Bc1g_01081 | bZIP transcription factor | BotBank project | Giesbert et al., *submitted to MPMI* |
| Bc1g_02686 | Regulator of photolyases | BotBank project | J. Schumacher & P. Tudzynski, *unpublished* |
| Bc1g_11672 | Microsomal signal peptidase 12kD subunit | BotBank project | J. Schumacher & P. Tudzynski, *unpublished* |
| Bc1g_03596 | Glycoside hydrolase family protein | BotBank project | J. Schumacher & P. Tudzynski, *unpublished* |
| Bc1g_10796 | Putative sterol glucosyltransferase | BotBank project | J. Schumacher & P. Tudzynski, *unpublished* |
| Δbtp1 | Transmembrane protein 1 (BTP1) [7-TM] | | Schulze Gronover et al. 2005 |
| Δbtp2 (Bc1g_05592) | Transmembrane protein 2 (BTP1) [7-TM] | BotBank project | A. Strotbaum & J. Schumacher, *unpublished* |
| Δbcgpr1 | G protein-coupled receptor 1 | cAMP signalling | A. Krüger & J. Schumacher, *unpublished* |
| Δbcgpr2 | G protein-coupled receptor 2 | cAMP signalling | A. Strotbaum & J. Schumacher, *unpublished* |
| Δbcgpr3 | G protein-coupled receptor 3 | cAMP signalling | A. Strotbaum & J. Schumacher, *unpublished* |
| Δbcgpr4 | G protein-coupled receptor 4 | cAMP signalling | A. Strotbaum & J. Schumacher, *unpublished* |
| Δbcgpr5 | G protein-coupled receptor 5 | cAMP signalling | A. Strotbaum & J. Schumacher, *unpublished* |
| Δbop1 | Opsin1 (7-TM) (BcSAK1-regulated) | Light sensing? | J. Heller & P. Tudzynski, *unpublished* |
| Δbcg1 (new) | Gα subunit 1 (BCG1) | cAMP signalling | Schulze Gronover et al. 2001 |
| Δbcg2 | Gα subunit 2 (BCG2) | cAMP signalling | Schulze Gronover et al. 2001 |
| Δbcg3 | Gα subunit 3 (BCG3) | cAMP signalling | Döhlemann et al. 2005 |
| Δbcgb1 (new) | Gβ subunit 1 (BcGB1) | cAMP signalling | J. Schumacher, *unpublished* |
| Δbcgg1 | Gγ subunit 1 (BcGG1) | cAMP signalling | J. Schumacher, *unpublished* |
| Δbac | Adenylatcyclase BAC | cAMP signalling | Klimpel et al. 2002 |
| Δbcpka1 | Protein kinase A - catalytic subunit 1 | cAMP signalling | Schumacher et al. 2008, MPMI |
| Δbcpka2 | Protein kinase A - catalytic subunit 2 | cAMP signalling | Schumacher et al. 2008, MPMI |
| Δbcpde1 | cAMP phosphodiesterase (low-affinity) | cAMP signalling | M. Knödler & B. Tudzynski, *unpublished* |
| Δbcpde2 | cAMP phosphodiesterase (high-affinty) | cAMP signalling | M. Knödler & B. Tudzynski, *unpublished* |
| Δbccnmp1 | cAMP-binding protein | cAMP signalling | M. Knödler & B. Tudzynski, *unpublished* |
| Δbpk2 | Sch9-like protein kinase | | Tudzynski & Schulze Gronover, 2004 |
| Δbpk3 | CLK1-like Ser/ Thr protein kinase | | Tudzynski & Schulze Gronover, 2004 |
| Δbpk4 | Ran1-like protein kinase | | Tudzynski & Schulze Gronover, 2004 |
| Δbcsnf1 | Protein kinase involved in C repression | | J. Schumacher & B. Tudzynski, *unpublished* |
| Δbcvel1 | Velvet 1 - Global regulator | | J. Schumacher, S. Traeger et al., *manuscript in prep* |
| Δbclae1 | Methyltransferase - Global regulator | | S. Traeger & B. Tudzynski, *unpublished* |
| Δbcwcl1 | White collar 1 homologoue (blue light receptor) | Light sensing | P. Canessa, J. Schumacher et al., *unpublished* |
| Δbccrz1 | Calcineurin-regulated transcription factor | Calcium signalling | Schumacher et al. 2008, Euk. Cell |
| Δbcrcn1 | Regulator of calcineurin (CN) | Calcium signalling | K. Harren & B. Tudzynski, *unpublished* |
| Δbcmid1 | Calcium channel protein | Calcium signalling | K. Harren & B. Tudzynski, *unpublished* |
| Δbccch1 | Calcium channel protein | Calcium signalling | K. Harren & B. Tudzynski, *unpublished* |
| Δbcmid1Δbccch1 | Calcium channel protein (double mutant) | Calcium signalling | K. Harren & B. Tudzynski, *unpublished* |
| Δbchk1 | Histidin kinase 1 | Sensor kinase | N. Temme & P. Tudzynski, *unpublished* |
| Δbchk5 | Histidin kinase 5 | Sensor kinase | J. v. Kan, *unpublished* |
| Δbctf1 | bZIP transcription factor | | N. Segmüller & P. Tudzynski, *unpublished* |
| Δbcatf1 | ATF1 transcription factor | | N. Temme & P. Tudzynski, *unpublished* |
| Δbcddr48 | DNA damage response (BcSAK1-regulated) | Stress response | J. Heller & P. Tudzynski, *unpublished* |
| Δbcsod1 | Cu-Zn-superoxide dismutase | ROS signalling | Rolke et al. 2004 |
| Δbcgod1 | Glucose oxidase | ROS signalling | Rolke et al. 2004 |
| Δbap1 | AP1-like transcription factor | ROS signalling | Temme & Tudzynski, 2009 |
| ΔbcnoxA | NADPH oxidase catalytic subunit A | ROS signalling | Segmüller et al. 2008 |
| ΔbcnoxB | NADPH oxidase catalytic subunit B | ROS signalling | Segmüller et al. 2008 |
| ΔbcnoxR | NADPH oxidase regulatory subunit | ROS signalling | Segmüller et al. 2008 |
| Δbcgo1 | Glyoxal oxidase | ROS signalling | J. Heller & P. Tudzynski, *unpublished* |
| Δbcpls1 | Tetraspanin (transmembrane protein) | ROS signalling?! | J. Heller & P. Tudzynski, *unpublished* |
| Δbcras2 | RAS-type GTPase BcRAS2 | Small GTPase | Schumacher et al. 2008, MPMI |
| Δbccdc42 | Rho-type GTPase BcCDC42 | Small GTPase | L. Kokkelink & P. Tudzynski, *manuscript in prep* |
| Δbcbem1 | Scaffold protein | (Small GTPase) | S. Giesbert & P. Tuduynski, *unpublished* |
| Δbcfar1 | Scaffold protein | (Small GTPase) | S. Giesbert & P. Tuduynski, *unpublished* |

**Table 3.5 Knock-out signaling mutants of *B. cinerea***. In the table the name of the mutant, the replaced gene, eventual comment about the signaling pathways and references are reported.

The mutants were grown on PDA plates for one week before conidia collection. DEFL 13 (at concentration of 50 μg/ml) was assayed *in vitro* in a 96 wells plate against each mutant and the percentage of conidia germination inhibition was calculated and compared to the wild type *B. cinerea* (following the protocol reported above). Each assay was indipendently repeated three times with three technical replicates for measurements.

### 3.3.8 Polyclonal antibody against DEFL 13: production, purification and Western Blot analysis

Polyclonal antibodies against DEFL 13 were produced by Primm srl by immunizing two rabbits with synthetic peptide conjugated to ovalbumin ($NH_2$-DGRCCKDHPKLGHCVP-COOH). Dilution series (1:50, 1:500, 1:5000 and 1:10000) of the two serum from rabbit 1 and 2 were tested in Western blot assay against the purified DEFL13. The serum from rabbit 1 was selected as the most specific and concentrated and was purified by CNBr-sepharose affinity (GE Healthcare), following the protocol recommended by Primm srl. Briefly, the serum was loaded on the CNBr-sepharose column (GE Healthcare ) previously coupled with the synthetic peptide and eluted with 100 mM Glycine, 500 mM NaCl, pH 2.5. The collected fractions were immediately buffered with Tris-HCl pH 8 to keep a physiological pH. Finally, each IgG eluted fraction was read at 280 nm.

Western blot analysis was conducted on 2.5 μg each of purified DEFL 13 and mutants. The peptides were separated on Tricine SDS gel with a low molecular weight marker (Novex, Invitrogen). The gel was electroblotted against a PVDF membrane (Hybond-P, American Biosciences) which was afterwards blocked for 1 h in blocking buffer (50 mM Tris-HCl, 150 mM NaCl, 0.1% (v/v) Tween 20 and 5% (w/v) of skimmed milk, pH 7.6) following overnight incubation with the purified primary antibody (diluited 1:100 in blocking solution).

Detection of wild type DEFL 13 and mutants was achieved with anti-rabbit IgG-Alkaline phosphatase secondary antibody (Sigma-Aldrich) and the BCIP/NBT (Sigma-Aldrich) staining solution (mixture of 5-bromo-4-chloro-3'-indolyphosphate p-toluidine salt and nitro-blue tetrazolium chloride), following the manufacturer's instructions.

### 3.3.9 DEFL 13 mutagenesis

*In vitro* site-directed mutagenesis was performed using "Quick change II site directed mutagenesis Kit" (Agilent Technologies) and the recombinant pOPIN M-*DEFL* 13 as template. For each mutation, two primers were designed (25-45 bases, Tm>78°C), annealing to the same sequence on opposite strand of the plasmid with the desiderate mutation in the middle of each primer (Table 3.6).

| Site-direct mutation | Primers (5'-3') |
|---|---|
| **W30A** | 1 CAAATGGTGGAAAATGTGCGACATATTGTATCAC |
| | 2 GTGATACAATATGTCGCACATTTTCCACCATTTG |
| **L42S** | 1 GTTCAAAGGGTGGCTGCTGCAAAAAATTATC |
| | 2 GATAATTTTTTGCAGCAGCCACCCTTTGAAC |
| **S48F** | 1 GGCTTATGCAAAAAATTATCTTTTGGTCGTCATGTTTGTCATTG |
| | 2 CAATGACAAACATGACGACCAAAAGATAATTTTTTGCATAAGCC |
| **S48K** | 1 GGCTTATGCAAAAAATTATCTAAGGGTCGTCATGTTTGTCATTG |
| | 2 CAATGACAAACATGACGACCCTTAGATAATTTTTTGCATAAGCC |
| **R50Q** | 1 CAAAAAATTATCTGGTGGTCAACATGTTTGTCATTG |
| | 2 CAATGACAAACATGTTGACCACCAGATAATTTTTTG |

**Table 3.6 Forward and reverse primers used for the site-directed mutagenesis**. The primers were synthesized HPLC-grade pure by PRIMM srl.

The PCR reactions were performed following the protocol provided with the kit. Briefly, the PCR reaction contained 10 ng of recombinant plasmid (pOPIN M-*DEFL* 13), 125 ng of each primer, 1 µl of dNTPs mix and 2.5 U of Pfu Ultra DNA polymerase. The PCR program was reported in the table 3.7.

| Segment | Cycles | Temperature | Time |
|---|---|---|---|
| 1 | 1 | 95°C | 30 sec |
| 2 | 16 | 95°C | 30 sec |
| | | 55°C | 1 min |
| | | 68°C | 7 min * |

**Table 3.7. PCR program for site-direct mutagenesis.** * The time was calculated considering about 1 min/Kb of plasmid length.

10 U of *DpnI* restriction enzyme were added directly to each amplification reaction and incubated at 37°C for 1 h. XL-1 Blue competent cells (Agilent Technologies) were transformed with *DpnI* treated samples and plated on ampicillin (100 µg/ml) LB plates. Positive colonies were inoculated in LB supplemented with ampicillin and used for plasmid preparation using Nucleospin Plasmid kit (Macherey-Nagel). The purified

plasmids were sequenced by BMR-genomics.

Plasmids containing the correct mutation were transformed into chemical competent *E. coli* SHuffle by heat shock. Plates were incubated for 18 h at 37°C before individual colonies were used to small scale expression test, following the protocol reported above for the other grapevine DEFLs. Pelleted cells from 3 l of bacterial cultures, able to express the recombinant soluble mutated protein, were resuspended in lysis buffer (50 mM Tris-HCl, 500 mM NaCl, 20 mM imidazole, 50 mM glycine, 20% (v/v) glycerol, pH 8) and lysed by sonicator (Bandelin Sonopul). Lysates were centrifuged at 18000 g for 30 min and the filtered (0.45 μm) supernatants were applied to pre-equilibrated 5 ml $Ni^{2+}$-IMAC columns (GE Healthcare) and proteins were eluted by imidazole gradient. Fractions containing fusion mutated protein were pooled, concentrated and dialyzed overnight against 20 mM HEPES, 150 mM NaCl, pH 7.5. The MBP-6xHis tag was removed by digestion with 3C protease (12 μg/mg of fusion protein) overnight at 4°C and injected onto a Superdex 75 column Hiload 16/60 (GE Healthcare) pre-equilibrated with 20 mM HEPES, 150 mM NaCl, pH 7.5. The fractions containing protein were pooled, concentrated and their purity was confirmed by SDS-PAGE gel. Proteins were quantified by their absorbance at 280 nm using the corresponding calculated ε (Protparam_http://web.expasy.org/protparam).

The purified mutants (W30A, L42S, S48F, S48K and R50Q) were tested for their ability to induce membrane permabilization in *B. cinerea* using the SYTOX green assay reported for DEFL 13.

# 4 RESULTS

## 4.1 Gene expression, antimicrobial activity and membrane interaction of the peach (*Prunus persica*) defensin PpDFN1

### *4.1.1* BLAST search of peach *DEFLs*

A BLAST search against the peach genome predicted peptides V 1.0 (http://www.rosaceae.org) using PpDFN1 as query, yielded seven sequences encoding for similar DEFLs (Figure 4.1). The corresponding genes have the conventional defensin structure with two exons separated by one intron. With exception of ppa013508, which lacks the signal peptide, they encode for DEFL precursor proteins with a typical signal peptide for extracellular localization followed by the mature peptide. The mature peptides are about 50 amino acids long and contain the DEFL hallmarks: eight conserved cysteines, CSαβ motif and γ-core signature (Figure 4.1). The identified mature peptides display a significant sequence identity with PpDFN1, ranging from 62% (ppa21088) to 72% (ppa16594). Based on the identity percentage, two groups of sequence can be identified: one comprises the peptide predictions ppa025677, ppa023476, ppa021088, ppa014119 and ppa019504, the other one comprises PpDFN1, ppa013508 and ppa016594 (Figure 4.1). Interestingly, as reported in the database, the first group are encoded by genes mapping on chromosome 7 of the peach genome and the *DEFL* sequences encoding the second group (including PpDFN1) cluster together on chromosome 1, suggesting that they have originated by recent local duplication events.

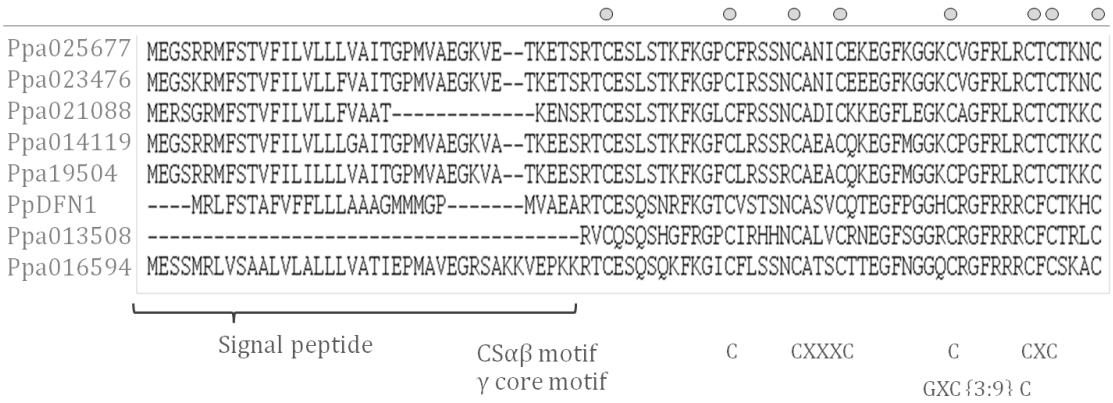


**Figure 4.1 Multiple sequence alignment of peach DEFLs**. Alignments were performed with CLUSTAL X. The signal peptides, the CSαβ motif and γ-core structural signature are highlighted. The conserved Cys residues are indicated by grey dots.

### 4.1.2 RT- qPCR analysis of Ppdfn1 gene expression

The level of *Ppdfn1* transcript was quantified by qPCR in different tissues (leaves, flowers and fruits at different ripening stages). *Ppdfn*1 transcript was always detectable by qPCR, suggesting a basal level of expression for this gene in all tissues. On the other hand, in flower, the gene expression of *Ppdfn1* was much higher than in the other tissues. This was calculated to be 4 times higher than in leaf and up to 33 times higher than in fruit at S1 ripening stage (Figure 4.2). In peach fruit, the *Ppdfn1* expression level does not vary during the early stages of ripening (S1 and S2) but drastically decreases from the pit hardening stage (the end of S2 phase) until the full ripeness (S4, climateric phase) (Figure 4.2). The inducibility of *Ppdfn1* upon pathogen infection was assayed in artificially inoculated peach fruits at S3 ripening stage with *Monilinia laxa* fungal pathogen. By comparing the level of *Ppdfn1* transcript in fungal and in mock infected fruits at 24 and 48 h post-inoculation, no significant variations were detected (data not shown), suggesting that the expression of this gene is not induced by this pathogen.

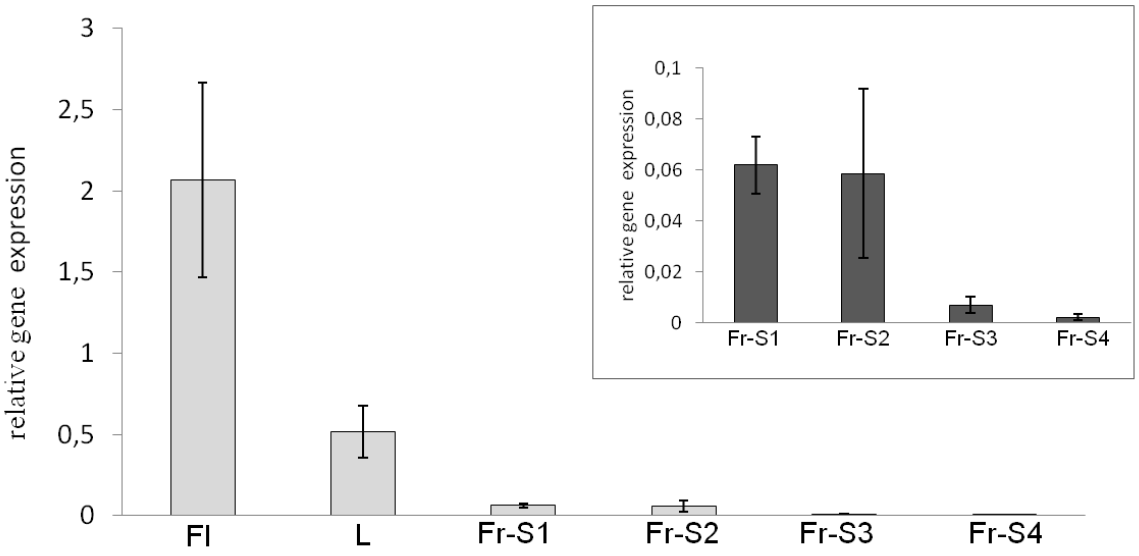


**Figure 4.2 Expression level of *Ppdfn1* in flowers (Fl), leaves (L) and fruits at different ripening stages (Fr-S1, Fr-S2, Fr-S3 and Fr-S4).** The small box is a zoomed view of the gene expression in S1-S4 fruits. Relative quantity of *Ppdfn1* target cDNA was normalized to the quantity of *actin* cDNA. Three replicates of each cDNA were synthesized from three different RNA extractions.

### 4.1.3 Cloning, expression and purification of PpDFN1

Mature PpDFN1 peptide, depleted of the predicted signal peptide, was produced as recombinant protein in *E. coli* Origami strain. This strain was selected for its ability to enhance the disulphide bond formation in the *E. coli* cytoplasm and is ideal for use with pET 32 vector, since the thioredoxin fusion tag further enhances the disulphide bonds formation. Recombinant protein was not expressed when *Ppdfn1* gene was cloned in pHAT plasmid, suitable for 6xHis fusion proteins (3 hours at 37°C or overnight at 20°C). On the other hand, cells transformed with recombinant pET32 vectors were able to express the fusion protein (TRX-6xHIS-PpDFN1). The fusion protein was expressed both also 37°C but at 20°C protein was expressed in higher quantity and solubility. After $Ni^{2+}$NTA affinity chromatography the fusion protein was digested with enterokinase proteinase and purified to homogeneity by cationic exchange chromatography (MONO-S) (Figure 4.3). The final yield was about 0.5 mg/l of bacterial culture.

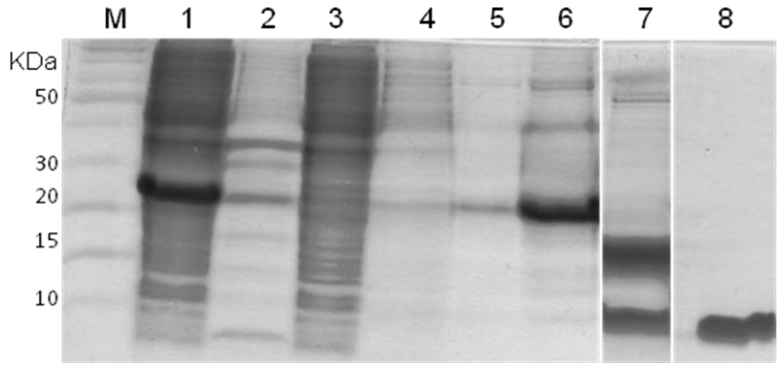


**Figure 4.3 SDS-PAGE of PpDFN1 expressed from *E.coli.*** M Protein marker; 1 soluble fraction of lysate *E. coli* cells transformed with pET32-*Ppdfn1* and induced by IPTG; 2 insoluble fraction of lysate *E.coli* cells transformed with pET32-*Ppdfn1* and induced by IPTG; 3 $Ni^{2+}$NTA column flow through; 4 and 5 20 mM of Imidazole column washes; 6 TRX-6xHis-PpDFN1 fractions eluted with 200 mM Imidazole; 7 soluble fractions after enterokinase cleavage; 8 MONO-S fraction of pure PpDFN1.

### *4.1.4* Antimicrobial activity of recombinant PpDFN1

Purified recombinant protein was used to test its antimicrobial activity against three fungi: *M. laxa*, *Botrytis cinerea* and *Penicillium expansum*. PpDFN1 antifungal activity was assayed by incubating fungal conidia with different concentration of the peptide and measuring the spectrophotometric absorbance of the fungal mass after 24, 48 and 72 h of incubation. PpDFN1 displayed a clear inhibitory effect on the growth of all three tested fungi. The strongest activity was shown against *P. expansum*: addition of 10 µg/ml of PpDFN1 lead to more than 90 % inhibition of *P. expansum* and about 74 % and 31 % inhibition of *M. laxa* and *B. cinerea* respectively (Figure 4.4). Consistently, the calculated IC50 values for PpDFN1 activity were 1.1, 15.1 and 9.9 µg/ml for *P. expansum, M. laxa* and *B. cinerea* respectively (Table 4.1). The microscopical analysis of treated fungi with PpDFN1 (data not shown) confirmed the lack of morphological alterations in fungal hyphae, as previously reported by Wisniewski (Wisniewski ME *et al.* 2003), classifying PpDFN1 as non morphogenic defensin.

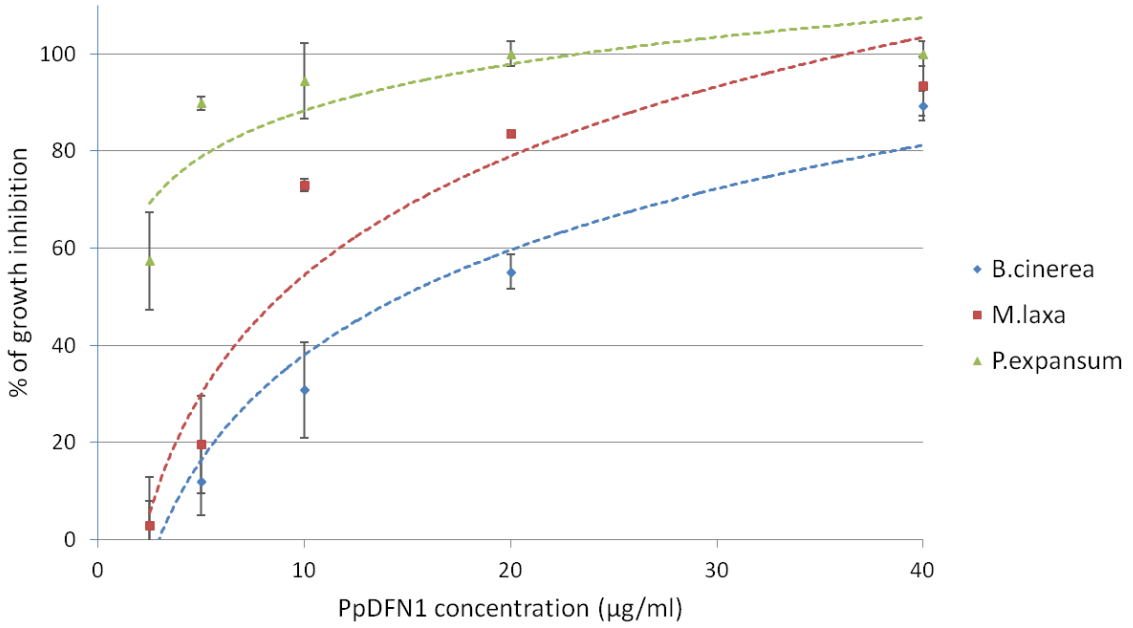


**Figure 4.4 Dose-response curves of PpDFN1 for *B. cinerea*, *M. laxa* and *P. expansum*.** Spectrophotometric readings of *B. cinerea*, *P. expansum* and *M. laxa* mycelial growth were taken after 72 h of incubation with 0-40 µg/ml of purified PpDFN1 at 20°C. The data are represented as a percentage of fungal growth as compared to the untreated control reaction with no peptide. Each data represents the average of three determinations ± standard error.

| fungus | IC50 (µg/ml) |
|---|---|
| *B. cinerea* | 15.1 |
| *P. expansum* | 1.1 |
| *M. laxa* | 9.9 |

**Table 4.1 IC50 values of the inhibition of the germination of *P. expansum*, *B. cinerea* and *M.laxa* conidia by PpDFN1.**

PpDFN1 did not exhibit antimicrobial activity (IC50 > 100 µg/ml) against bacterial plant pathogens, such as *Xanthomonas campestris*, *Psedumonas auroginosa*, and *Agrobacterium tumefaciens*, nor against the human pathogens *Listeria monocitogenes* and *Salmonella enteritidsi*. Similarly, no inhibitor effect was detected against the yeast *Saccharomyces cerevisae* (data not shown). Furthermore, toxicity of PpDFN1 against mammals was investigated through *in vitro* test against human erythrocyte, showing that the peptide did not display any haemolytic action (data not shown).

### *4.1.5* Fluorescence microscopy analysis

In order to determinate if the PpDFN1 antifungal activity involves fungal membrane permeabilization, a SYTOX green assay was performed on the sensitive fungi. When membranes are destabilized, this dye enters the cells and, upon binding to DNA, increases its fluorescence. PpDFN1 clearly induced SYTOX green uptake in *B. cinerea* and *M. laxa* cells where, after 6 h of protein incubation, nuclei become highly fluorescent (Figure 4.5). On the other hand, at the same condition, the degree of SYTOX green uptake in *P. expansum* cells appears much weaker. Despite the fluorescence microscopy analysis can not be considered a quantitative assay, this result suggests a lower degree of membrane destabilization in *P. expansum*.

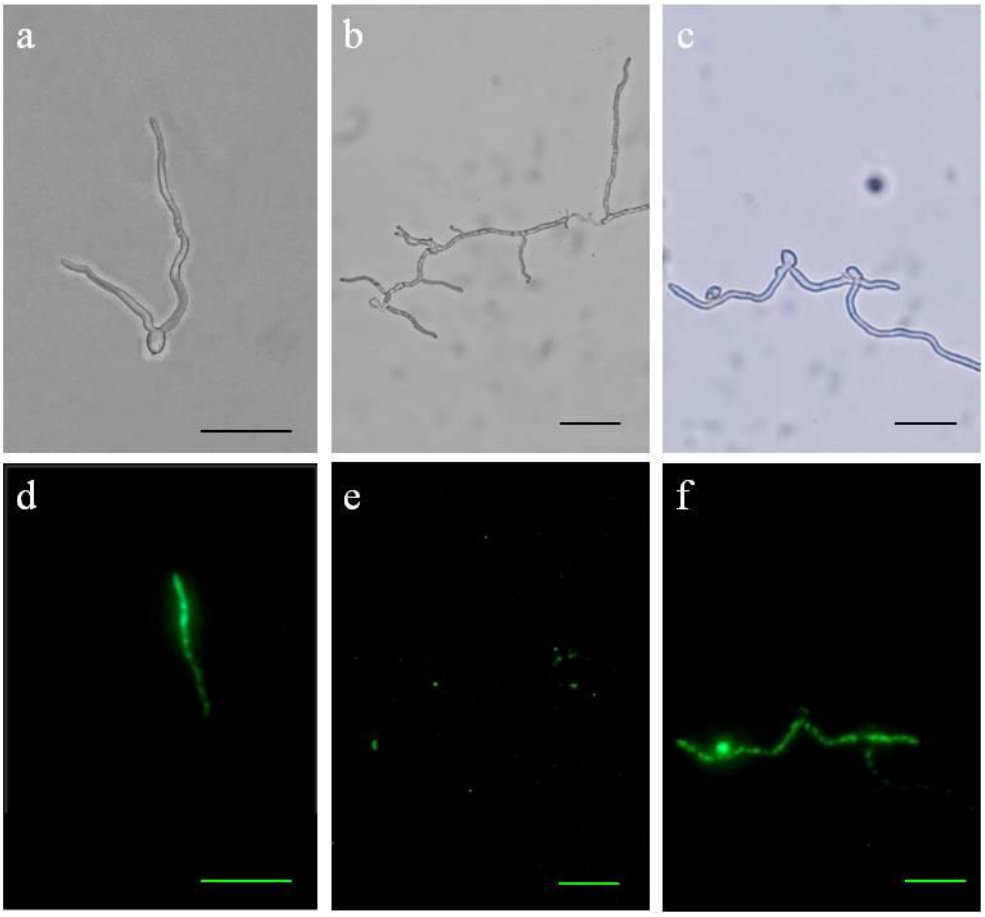


**Figure 4.5 SYTOX green uptake by fungal hyphae treated with PpDFN1**. Fungal hyphae of *B. cinerea* (a and d), *P. expansum* (b and e) and *M. laxa* (c and f), were incubated with 1µM of SYTOX green and 40 µg/ml of PpDFN1. Bright field images (a, b, c) and fluorescence microscopy images (d, e, f). The results of membrane permeabilization are representative of one triplicate experiment. Bar= 50µm

### *4.1.6* Monolayer measurements

PpDFN1 localized on the surface of treated fungal hyphae, as shown by our collaborators of Institute of Biophysical (CNR, Trento Italy) with confocal experiments and FITC-labeled PpDFN1 (Nanni V and Zanetti M *et al.* paper submitted). Considering that PpDFN1 stays localized for hours on the surface of fungi and causes membrane permeabilization, we decided to investigate the interaction between the peptide and the lipids by Langmuir monolayer technique. Lipid films, generated both with commercial lipids and lipids extracted from *M. laxa*, *B. cinerea* and *P. expansum* were assayed. The ability of PpDFN1 to insert into lipid films is dependent on the film lipid composition (Figure 4.6): PpDFN1 does not insert into pure egg-phosphatidylcholine (ePC) monolayers, nor into films obtained with lipids extracted from human erythrocytes (RBC, red blood cell), in accordance with hemolytic tests. However, when ceramide β-D-galactoside, a component of glycosphingolipid family, is added to the ePC lipid film, an increase in surface pressure is measured. The highest rate of the surface pressure increase was obtained with lipids extracted from fungi, indicating the PpDFN1 preference for these natural lipids. Interestingly, PpDFN1-lipids binding well correlated with the calculated IC50 values, with the strongest interaction shown for *P. expanusm.*

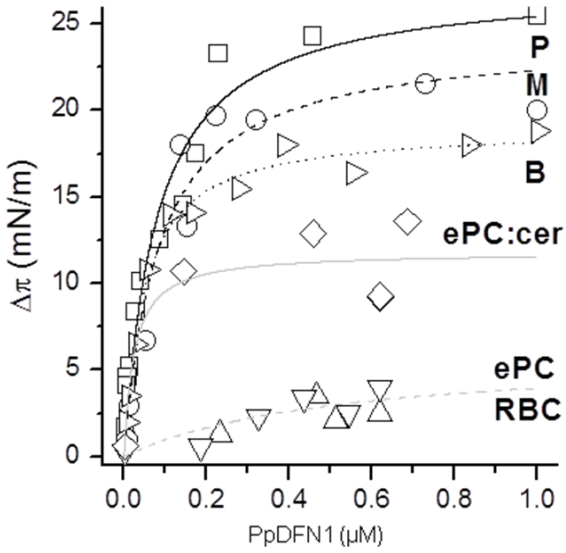


**Figure 4.6 Titration measurements on different lipid monolayers**. Monolayers were composed of: egg-phosphatidylcholine (ePC); ePC and ceramide β-D-galactoside in 2% molar ratio (ePC:cer); total lipids extract of *P. expansum* (P); total lipid extract of *M. laxa* (M); total lipid extract of *B. cinerea* (B); total lipid extract of human red blood cells (RBC). The initial pressure was set up at 20 mN/m in 10 mM Hepes, 50 mM

KCl, 0.1 mM EDTA, pH 7. The surface pressure π of the lipid monolayer is defined as the decrease in surface tension γ, i.e., $\pi = (\gamma_o - \gamma_m)$ , where $\gamma_m$ and $\gamma_o$ represent the surface tension of the water/air interface in the presence or absence of the lipid monolayer.

## 4.2 Identification and characterization of the defensin-like gene family in grape (*Vitis vinifera*)

### 4.2.1 Genome identification of *DEFL* sequences and analysis of their primary structure

A screening of the *Vitis vinifera* genome, carried out in the laboratory of Dr. Claudio Moser at IASMA (Research and Innovation Center, Edmund Mach Foundation, San Michele all'Adige, Trento. Italy), lead to the identification of 79 *DEFL* sequences, which were numbered from 1 to 79 (Giacomelli *et al.* paper submitted). They consist of 46 genes and/or allelic variants, 9 likely pseudogenes and 24 gene fragments. Considering their cysteine signatures, the encoded grape DEFLs were separeted in four groups as shown in Figure 4.7. Although the sequences included in group 1 and 3 share low intra-group similarity, they all share a conserved pattern of cysteine residues. On the contrary, sequences of group 2 are extremely conserved and they are the most abundant. The other identified DEFLs are highly heterogeneous and, with exclusion of the CSαβ motif, lack any peculiar cysteine hallmark arrangement. They were all grouped in a fourth additional DEFL group.

Group 1: $CX_{3-14}CX_{4-5}CX_3CX_{8-11}CX_{5-10}CCC$

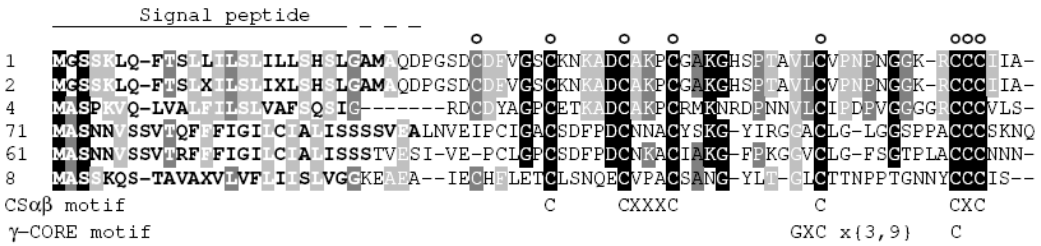

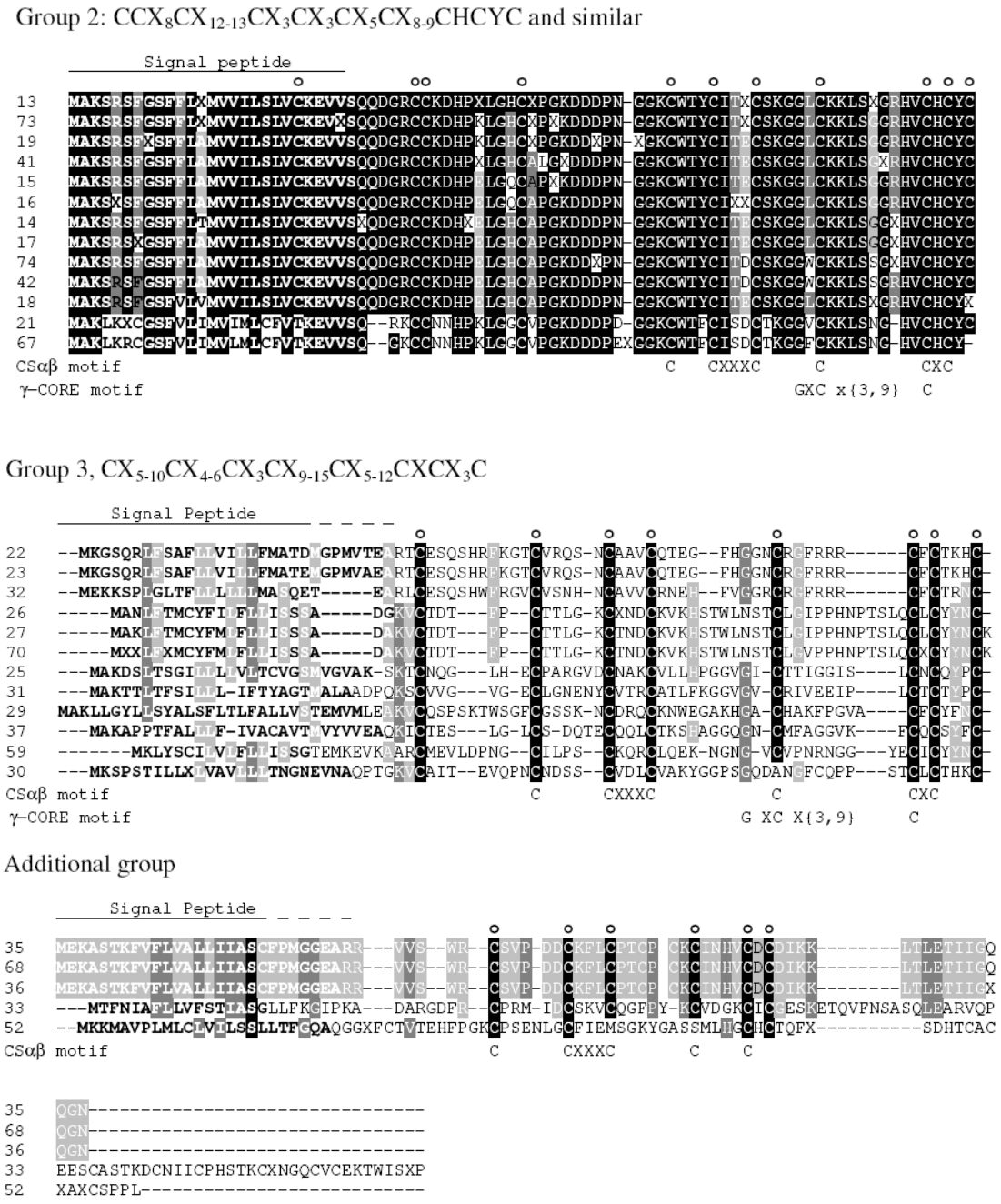


**Figure 4.7 Multiple sequence alignments of grapevine DEFLs according to their cysteine signature**. Sequence have been classified in three groups according to the specific cysteine pattern. The additional group includes all other DEFLs which are not comprised in group 1, 2 or 3. The position of conserved cysteine is indicated by small circles above the alignments. Uncertain amino acids are indicated by x. Sequence similarity is highlighted by different grey tonalities, lighter for low similarity up to black for aminoacid identity. The signal peptide as predicted with signalP is indicated in bold.

All sequences in **group 1**, with the exception of gene fragments, translate into peptides containing the distinctive CSαβ motif , γ-core signature and the predicted signal peptide positioned at their N-terminus. These sequences display a number of cysteine

residues in the mature protein varying from eight to ten, and a $CX_{3-14}CX_{4-5}CX_3CX_{8-11}CX_{5-10}CCC$ pattern. **Group 2** includes 13 translated *DEFL* gene sequences. These consist of highly conserved basic peptides, containing nine or ten cysteine residues arranged in CSαβ and γ-core motif. All DEFL peptides included in this group share a typical cysteine pattern $CCX_8CX_{12-13}CX_3CX_3CX_5CX_{8-9}CHCYC$, with the exception of DEFL 18 and 67, lacking the last cysteine residue. **Group 3** collects sequences displaying the conserved cysteine pattern $CX_{5-10}CX_{4-6}CX_3CX_{9-15}CX_{5-12}CXCX_3C$ all containing the CSαβ signature. Group 3 includes the *Vitis vinifera Antimicrobial peptide 1* (*Vv-Amp1*) (de Beer A and Vivier MA 2008), which is the only grapevine defensin gene characterized so far. Finally, nine *DEFLs* genes and 11 fragments were ascribed to the additional group (**group 4**)

### 4.2.2 Selection of grape *DEFLs*, recombinant expression, purification and antimicrobial activity

The genomic structure and organization of *DEFL* gene family was known only for herbaceous species, such as *Arabidopsis thaliana*, *Medicago truncatula* and *Oryza sativa*; *Vitis vinifera* is the first (and so far the only one) woody plant species for which this knowledge has been achieved. Before this study, only the defensin VvAMP1 has been characterized in this species (de Beer A and Vivier MA 2008).

During the course of this PhD work, the grapevine *DEFL* gene family was studied also at the transcriptome level by the laboratory of Dr. Moser (Giacomelli L *et al.* paper submitted). The expression of the 46 identified *DEFL* genes was evaluated by RT-qPCR indicating that many of grapevine *DEFL* genes were specifically expressed in different tissues and at different stages, for examples the expression of *DEFL* 31, 61 and 71 is detectable only in immature seeds and *DEFL* 59 and group 2 appeared to be predominant expressed in inflorescence tissue. In order to elucidate the possible role of *DEFLs*, Giacomelli L *et al.* (paper submitted ) investigated also the expression induction upon *B. cinerea* infection. Some *DEFL* genes resulted up regulated in challenged fruits and inflorescences. On the basis of these results we decided to characterize the activity of some grapevine DEFL proteins. DEFL candidates were selected with the intention to have representative sequence of each group (1-2-3), possibly expressed with a different pattern. Upon these considerations, the sequences encoding for the mature forms of DEFL 1 (group 1), 13 (group 2), 22, 31 and 59 (group 3) were selected for heterologous expression (Table 4.2).

| DEFL | GROUP | *DEFL* expression in grapevine tissues | | | | Mature peptide | |
|---|---|---|---|---|---|---|---|
| | | S | I | I + *B. cinerea* | F | MW | pI |
| **1** | 1 | X | X | | | 5037,80 | 8,20 |
| **13** | 2 | | | X | | 6242,2 | 8,38 |
| **22** | 3 | | | | X | 5355,0 | 9,37 |
| **31** | 3 | X | | | | 5400,3 | 5,01 |
| **59** | 3 | | X | | | 4297,1 | 8,19 |

**Table 4.2 Gene expression of *DEFL* 1, 13, 22, 31, and 59, and molecular weight and isoelectric point of the encoded DEFL products**. Seed (S), inflorescence (I), I + *B. cinerea* (inflorescence upon artificial *B. cinerea* infection) and fruit (F) are the tissues where the gene expression was evaluated by RT-Real Time PCR (Giacomelli *et al.* paper submitted). MW=molecular weight, pI=isoelectric point. These parameters were calculated using Protparam (http://web.expasy.org/protparam).

Different expression plasmids were used to test expression and solubility of these DEFLs (Table 4.3). In general, the expression of grapevine DEFLs was feasible only as fusion form of thioredoxin (in plasmid pET32) for VvAMP1, or maltose binding protein (in plasmid pOPIN M) for the other DEFLs. Expression and solubility yields were higher when carried out at 20°C overnight. Recombinant expression was never obtained for the DEFL 1 in any of tested conditions, therefore no members of group 1 DEFL were obtained.

| DEFL | Vector | Expression conditions | Protein expression | Protein solubility |
|---|---|---|---|---|
| **1** | pOPIN F | 37°C x 3 hours | X | |
| | | 20°C overnight | X | |
| | pOPIN M | 37°C x 3 hours | X | |
| | | 20°C overnight | X | |
| **13** | pOPIN F | 37°C x 3 hours | X | |
| | | 20°C overnight | X | |
| | pOPIN M | 37°C x 3 hours | √ | yes |
| | | 20°C overnight | √ √ | yes |
| **22** | pHAT | 37°C x 3 hours | X | |
| | | 20°C overnight | X | |
| | pET32 | 37°C x 3 hours | √ | yes |
| | | 20°C overnight | √ √ | yes |
| **31** | pOPIN F | 37°C x 3 hours | X | |
| | | 20°C overnight | X | |
| | pOPIN M | 37°C x 3 hours | √ | yes |
| | | 20°C overnight | √ √ | yes |
| **59** | pOPIN F | 37°C x 3 hours | X | |
| | | 20°C overnight | X | |
| | pOPIN M | 37°C x 3 hours | √ | yes |
| | | 20°C overnight | √ √ | yes |

**Table 4.3 Expression screening of selected grapevine DEFLs**. All tested vectors express for 6xHis fusion proteins at the N-terminus. The *DEFL* 22 (VvAMP1) cDNA was cloned in the vectors pHAT and pET32. pET32 encodes 6xHis and thioredoxin (TRX) tag. The *DEFLs* 1, 13, 31 and 59 were cloned in the vectors pOPIN F and pOPIN M. pOPIN M expresses for protein fused to maltose binding protein (MBP). Expression conditions = condition of protein expression upon IPTG induction. Protein expression = protein expression as observed by the band intensity in SDS-PAGE gel; lack of expression is indicated by an X, expression by a √ and major expression by √ √. Protein solubility = "yes" indicates the presence of the protein in the soluble fraction of *E. coli* upon cell lyses and centrifugation (determined by SDS-PAGE gel).

After affinity chromatography the fusion proteins were digested with enterokinase peptidase (for DEFL 22) or 3C protease (for DEFL 13, 31 and 59) and purified to

homogeneity by size exclusion chromatography (Figure 4.8). For all DEFLs, the final yield was about 0.2 mg/l of bacterial culture.

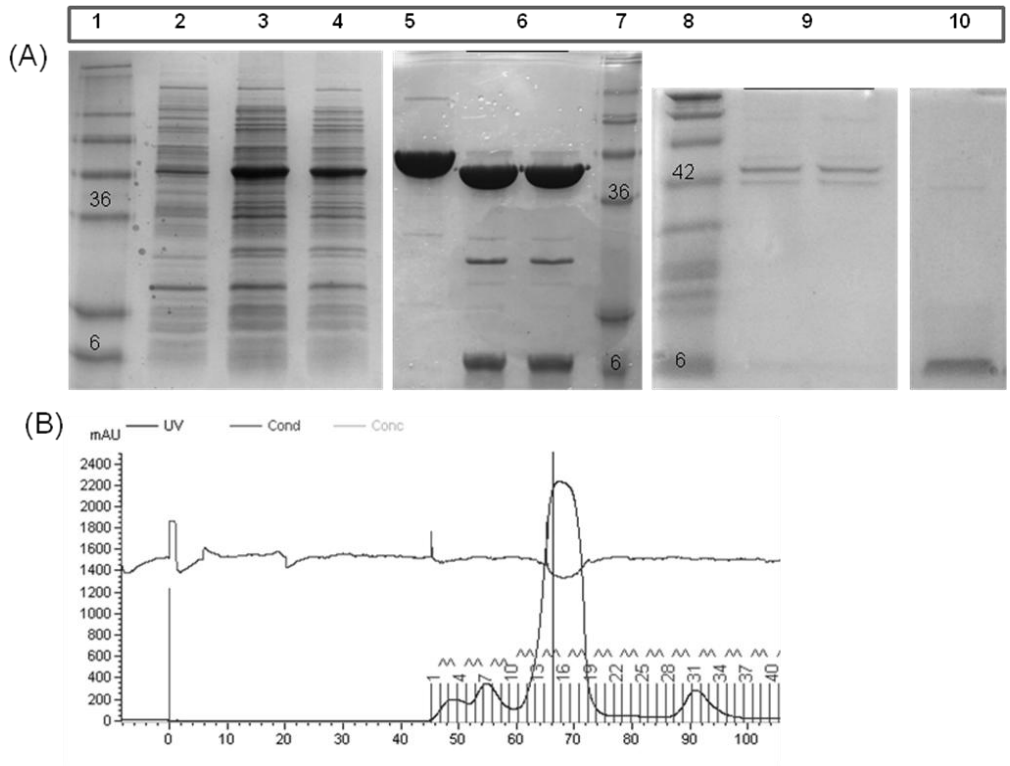


**Figure 4.8 SDS-PAGE and size exclusion chromatography of DEFL 13 (A) SDS-PAGE**; 1 protein marker; 2 *E. coli* BL21 transformed with pOPINM-*DEFL* 13 vector not induced (negative control); 3 Total and 4 soluble fraction of *E. coli* lysate trasformed with pOPINM-*DEFL* 13 vector induced by 0.4 mM of IPTG; 5 MBP-6xHis-DEFL 13 after affinity chromatography; 6 MBP-6xHis-DEFL 13 after 3C protease cleavage; 7 protein marker; 8 protein marker; 9 fraction eluted from size exclusion chromatography corresponding to the MBP-6xHis and 10 DEFL 13. (**B) Chromatogram of size exclusion protein purification**. In the y axis is reported the mAU at 280 nm and in the x axis the volume of elution. The recombinant DEFLs eluted at about 90 ml volume in Superdex 75 -16/60 column. Similar results were obtained for the other DEFLs.

The Ellman's test performed for the purified DEFLs 13, 22, 31 and 59 indicated the absence of free thiol groups, supporting the hypothesis that all cysteines in the primary sequences are engaged in disulphide bridges.

The chromatography techniques to purify grapevine DEFLs were performed in the biochemistry laboratory of Dr. Mark Banfield (John Innes Centre, Norwich. UK).

The purified recombinant DEFLs were tested for their antimicrobial activity against the causal agent of grey rot, *Botrytis cinerea*. The *in vitro* test was conducted incubating *B. cinerea* conidia with different concentration of DEFLs and observing the germination by

microscopy analysis. The IC50 values were calculated by spectrophotometric measurements. The microscope analysis of *B. cinerea* conidia showed that all recombinant DEFLs (13, 22, 31 and 59) significantly inhibited conidia germination with a different intensity. The mycelium showed no apparent alteration in hyphal morphology with respect to the untreated fungal culture (Figure 4.9). The IC50 values of 13, 22, 31 and 59 DEFLs were 5.3, 14.0, 30.4 and 50 µg/ml respectively (Table 4.3), indicating DEFL 13 as the strongest inhibitor. The IC50 value for DEFL 22 (previously named VvAMP1) was in the same order of magnitude previously reported by de Beer A and Vivier MA (de Beer A and Vivier MA 2008). When the same experiment was repeated using a reduced and alkylated form of the recombinant proteins, no significant differences in fungal growth, compared to the negative control, were observed (Figure 4.9). This indicates that the antimicrobial activity is strictly dependent on the oxidized form of the protein and that the intra-molecular disulphide bridges play a crucial role for the protein activity.

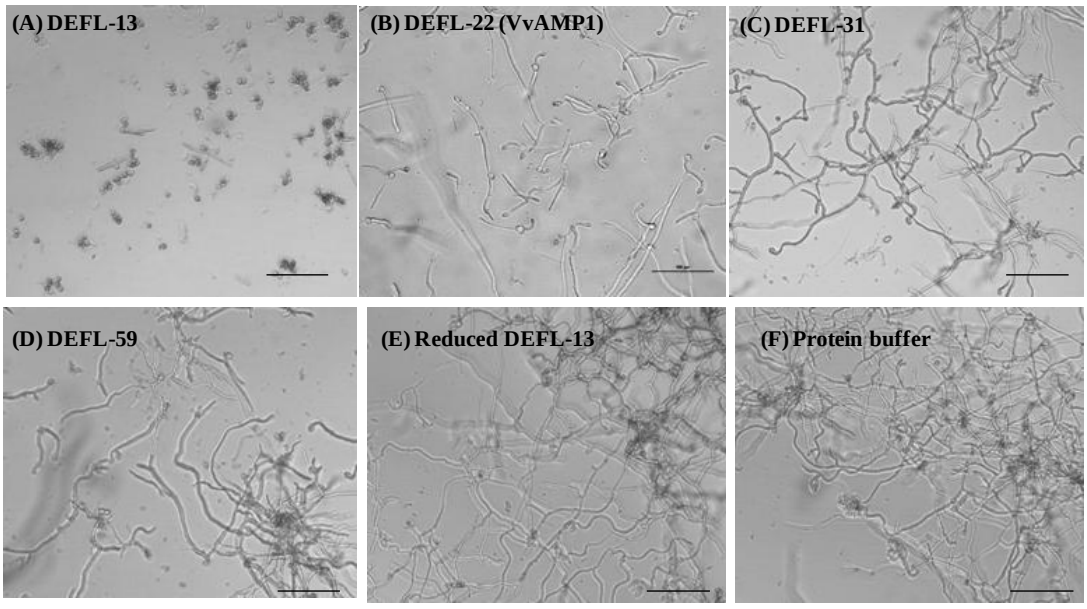


**Figure 4.9 Effect of the recombinant grapevine DEFLs on *B. cinerea* conidia germination**. Inhibition of *B. cinerea* conidia germination by (A) 50 µg/ml of DEFL 13, (B) 50 µg/ml of DEFL 22 (VvAMP1), (C) 50 µg/ml of DEFL 31, (D) 50 µg/ml of DEFL 59, (E) 50 µg/ml of reduced and alkylated DEFL 13 (similar results were obtained for the reduced and alkylated DEFL 22, 31 and 59) and (F) Protein buffer used as negative control. Bar = 100 µm

| DEFL | IC50 (µg/ml) |
|---|---|
| **13** | 5.3 |
| **22** | 14.0 |
| **31** | 30.4 |
| **59** | 50.0 |

**Table 4.3 IC50 values calculated for the different grapevine DEFLs inhibitory activity on the germination of *B. cinerea* conidia.**

## *4.3* Characterization of the antimicrobial activity of DEFL 13 from *Vitis Vinifera*

DEFL 13 was chosen in order to investigate on its antimicrobial activity, since displayed the lowest IC50 value against *B. cinerea* among the studied DEFLs. This one, as all group 2 DEFL, shows a different cysteine pattern compared to the one contained in the other plant defensins so far characterized.

### 4.3.1 Optimization of recombinant DEFL 13 expression and purification

With the aim to increase the yield of pure DEFL 13 obtained from *E. coli* expression, different expression, purification strategies and protocols were tried. Indeed, while the fusion protein form of MBP-6xHis-DEFL 13 in *E. coli* was produced with an yield of about 10 mg/l of bacterial culture, final yield in pure native DEFL 13 was only 0.2 mg/l of bacterial culture, indicating that much of the protein product was lost during purification after protein cleavage.

The recombinant expression in a eukaryotic host was tried in order to facilitate the formation of disulphide bridges, predicted to be 5 in a 57 amino acids-long peptide. The yeast *Pichia pastoris* was chosen. Ten different colonies of *P. pastoris* transformed with pPICZα-*DEFL* 13 were screened and no colony appeared to express protein in the extracellular environment nor in the cytoplasm. This was confirmed by SDS gel stained with InVision™ His-tag In-gel Stain, a fluorescent stain formulated for sensitive and specific detection of His-tagged fusion proteins.

In attempt to increase the protein production in *E. coli* system, the *E. coli* SHuffle

strain was shown to be a valid alternative to BL21 Origami strain, since the final yield in pure DEFL 13 was about 0.5 mg/l. (Table 4.4). SHuffle is an engineered *E. coli* strain capable of expressing, in the cytoplasm, proteins with high number of disulphide bridges, thanks to the presence of disulphide bond isomerase (DsbC). Furthermore, DsbC act also as general chaperone for protein folding. Probably the ability of Origami strain cells to enhance the expression of proteins rich in disulphide bonds is strictly associated with the presence of thioredoxin as protein fusion tag.

| ***E.coli* strain** | **Yield for liter of bacterial culture** |
|---|---|
| BL21 Origami | 0.2 mg/l |
| SHuffle | 0.5 mg/l |

**Table 4.4 Yields in purified DEFL 13 (mg/l of bacterial culture) expressed in two different *E. coli* strains.**

Trials to improve yield were made also by changing chromatography purification strategies, for example using $Ni^{2+}$NTA and amylose affinity chromatography (connected in series) after 3C protease cleavage (data not shown) or cation exchange chromatography, both instead of size exclusion as final purification step. These strategies allowed to achieve higher protein yield, however this was affected by lower purity level (Figure 4.10), unsuitable for *in vitro* function investigations.

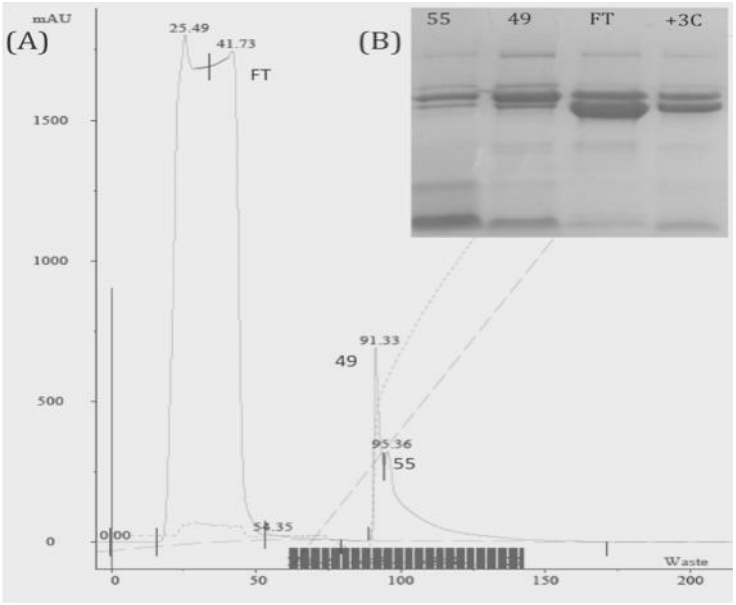


**Figure 4.10 Cationic exchange chromatography after 3C protease cleavage of MBP-6xHis-DEFL 13** (A) Cationic exchange chromatography of DEFL 13. FT is the column flow through peak; peaks 49 and 55 eluted respectively at 360 and 390 mM NaCl. (B) SDS page of cationic exchange chromatography. +3C, protein mixture after the 3C protease cleavage loaded in the SP sepharose column; FT, flow through; 49 and 55, eluted fractions.

### *4.3.2* Antimicrobial activity against fungal and bacterial pathogens

In order to analyse the spectrum of DEFL 13 action, the protein was assayed against a panel of different fungal pathogens and two bacterial plant pathogens. These were *Colletotrichum acutatum*, *Fusarium oxysporum*, *Monilinia laxa*, *Aspergillus niger*, *Alternaria arboresca*, *Penicillium expansum* and *Trichoderma spp.*. Fungal conidia were incubated with 50 ug/ml of peptide and germination was analysed by microscopy after 16 h (Figure 4.11 (1)). The percentage of fungal growth inhibition was calculated by spettrophotometric reading after 48 h as reported above (Figure 4.11 (2)). At 50 ug/ml concentration, DEFL 13 was able to inhibit more than 90% of *B. cinerea* growth and the growth of *C. acutatum*, *F. oxysporum*, *M. laxa*, *A. niger*, *A. arboresca*, *P. expansum* and *Trichoderma spp.* of 24.6, 22.0, 35.6, 62.7, 49.1, 10.3 and 26.8 % respectively, compared to untrated fungal conidia. All tested fungi did not show any morhological change respect to the untreated fungal hyphae, classifying the peptide as non morphogenic defensin.

(1)

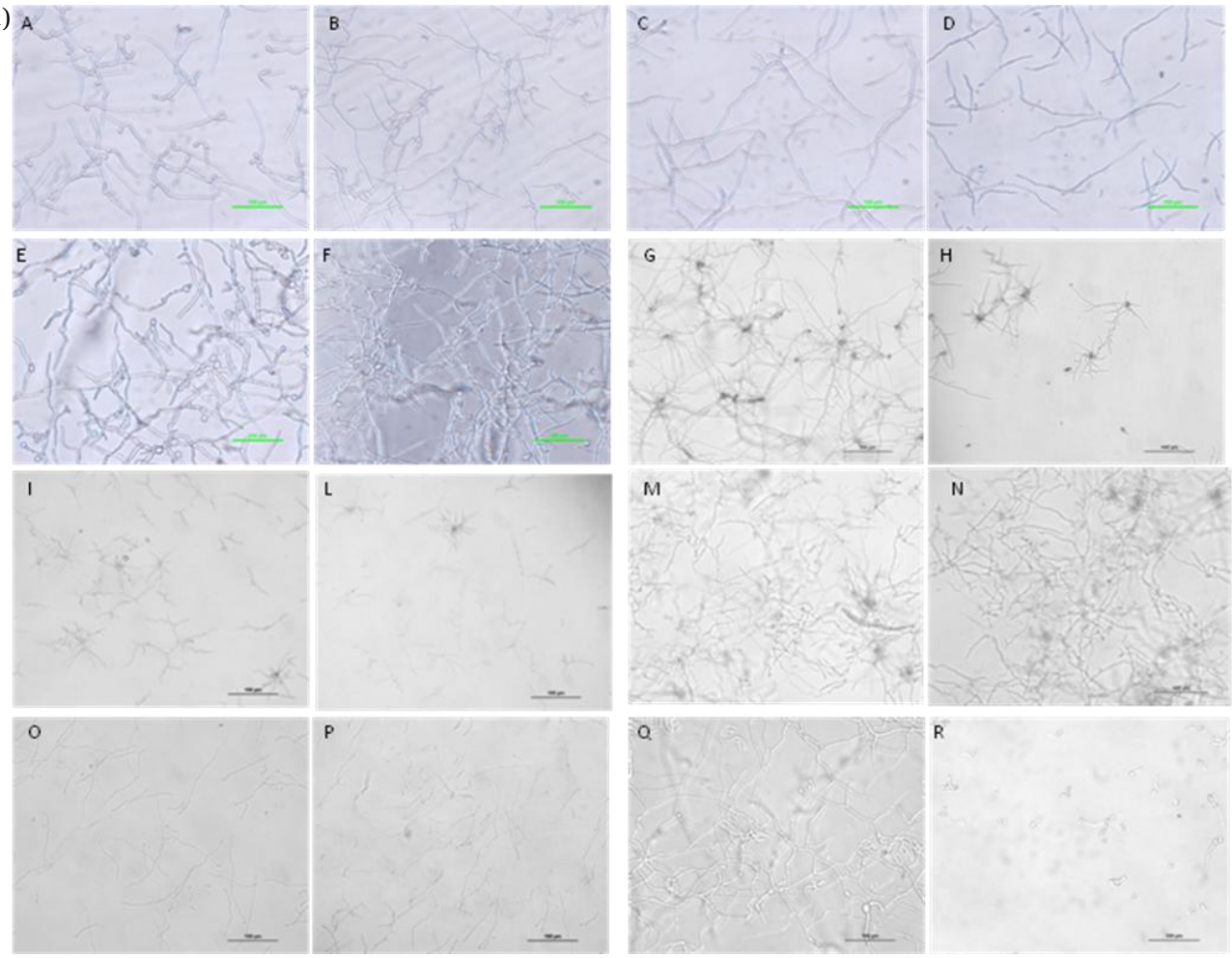


(2)

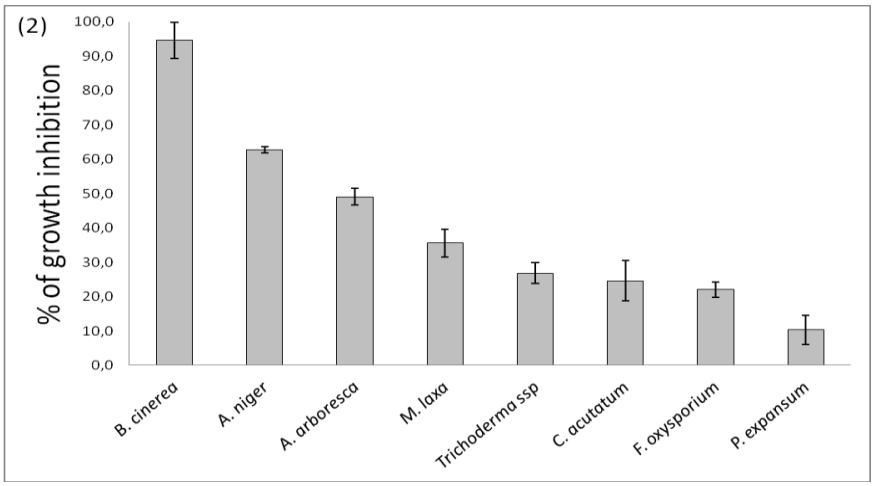


**Figure 4.11 Effect of DEFL 13 on a panel of fungi**. (1) Microscopy pictures of treated and untreated conidia. Microscopy analysis of conidia untreated (A, C, E, G, I, M, O, Q) and treated (B, D, F, H, L, N, P, R) with 50 ug/ml of DEFL 13, after 16 hours of incubation. (A, B) *Colletotrichum acutatum* (C, D) *Fusarium oxysporum* (E, F) *Monilia laxa* (G, H) *Aspergillus niger* (I, L) *Alternaria arboresca* (M, N) *Penicillium expansum* (O, P) *Trichoderma ssp* and *B cinerea* (Q, R). (2) Effect of DEFL 13 on fungal biomass. Spectrophotometric readings were taken after 48 h and compared to the untreated control reactions with protein buffer. Data are represented as % of fungal growth inhibition. The experiments were repeated three times and the standard deviation is reported on the graph.

Concentration up to 100 µg/ml of DEFL 13 did not provoke any effect on the growth of plant pathogenic bacteria *Agrobacterium tumefaciens* and *Erwinia amylovora* (data not shown).

### *4.3.3* Effect of the cations on the antifungal activity

The antifungal activity of some plant defensins is significantly reduced when the ionic strength of the fungal growth medium is increased. The effect of $K^+$ and $Mg^{2+}$ cations on the DEFL 13 antibotrytis activity was assayed by incubating *B. cinerea* conidia with different concentration of peptide (50, 25, 12.5, 6.25 and 3.13 µg/ml) in half PDB medium supplemented with different concentration of cations (50 mM, 25 mM and 12.5 mM for KCl and 5 mM, 2.5 mM and 1.25 mM for $MgCl_2$). The ability of DEFL 13 to inhibit the growth of *B. cinerea* strongly depends on cation concentration of the medium. In KCl supplemented medium (Figure 4.12 A) the percentage of inhibition gradually decreases as the cation concentration increases, showing a cation-dose dependence effect on antifungal activity at all tested peptide concentrations. This dependence is lost when a low concentration of DEFL 13 (3.13 µg/ml) is used but probably at this concentration the signal : noise ratio is too low to be considered reliable, as indicated by the scarce reproducibility of values found across different experiments (data not shown). The addition of $MgCl_2$ to the medium (Figure 4.12 B) strongly reduces the activity of the peptide: 5 mM of $MgCl_2$ is sufficient to completely abolish the antifungal effect of high concentration of DEFL 13 (50 µg/ml).

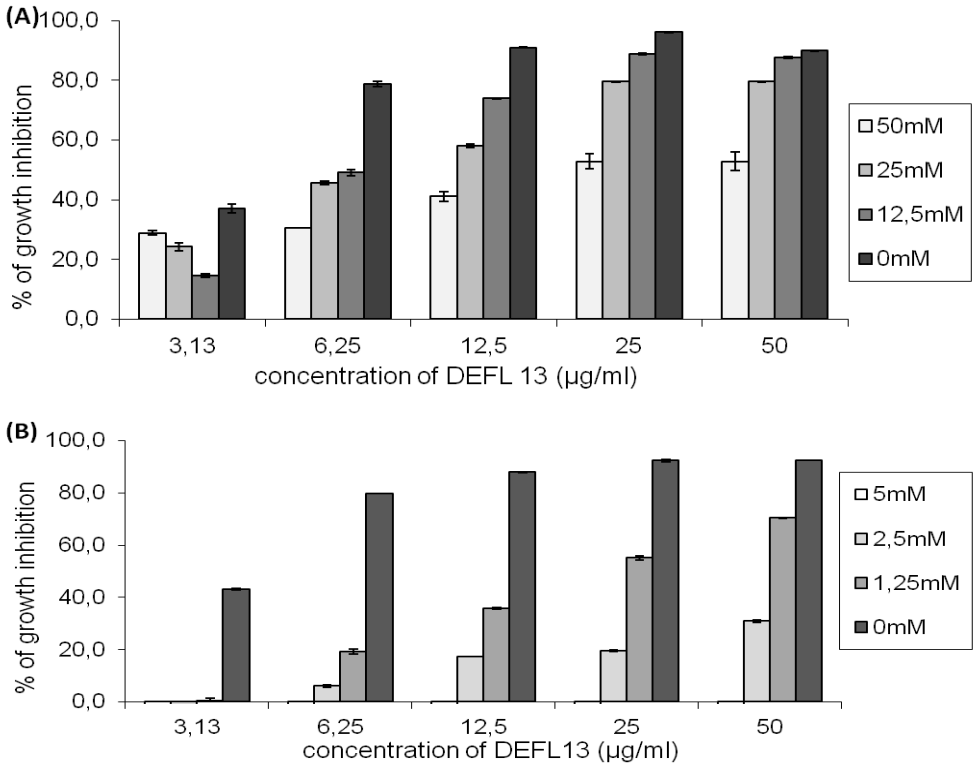


**Figure 4.12 Effect of different concentration of KCl (A) and $MgCl_2$ (B) on the antifungal activity of DEFL 13 agaisnt *B. cinerea*.** The % of growth inhibition and the concentration in µg/ml of DEFL 13 were reported in the y and x axis respectively. The different bar colors indicate the different medium as reported in the legend. Mean values and standard errors calculated on three replicates are reported on the graph.

### *4.3.4* Thermal stability of DEFL 13

The structural and functional stability of antimicrobial peptides at high temperatures is an important factor for their possible exploitation. For this reason, the thermal stability of DEFL 13 was assayed by circular dichroism (CD) spectroscopy. Far UV CD spectra of thermally treated DEFL 13 (10 min at 90°C) was compared to the one of the untreated DEFL 13. Furthermore, thermal treated peptide was assayed for its antifungal activity against *B. cinerea*.

The far UV CD spectrum of DEFL 13 at room temperature showed the presence of a significant amount of coiled structures (Figure 4.13) as indicated by the absence of the typical positive signals of α-helix and β-sheet secondary structures. The result of fits averaging provided a secondary structure composition of 16% α-elix, 26.5 % β-strand, 14.5 % turn and 42.9 % random coil. The spectra of untreated and thermal treated DEFL 13 did not display any significant difference, indicating that the secondary structure did not vary after a high temperature treatment (data not shown). Similarly, CD spectra did not vary

when the peptide was treated with DTT (dithiothreitol) reducing agent.

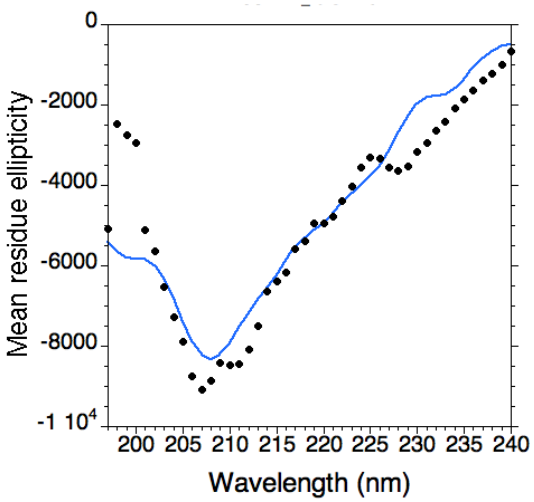


**Figure 4.13 Far-UV CD spectrum of DEFL 13**. Ten spectra were accumulated from 190 to 240 nm at 0.2 nm intervals and averaged to achieve an appropriate signal : noise ratio. The spectrum of the buffer was substracted.

Furthermore, when assayed in standard antibotrytis test, thermally treated DEFL 13, retained 30% of activity against *B. cinerea* conidia germination (compared to the 94% activity shown by untreated protein) (Figure 4.14).

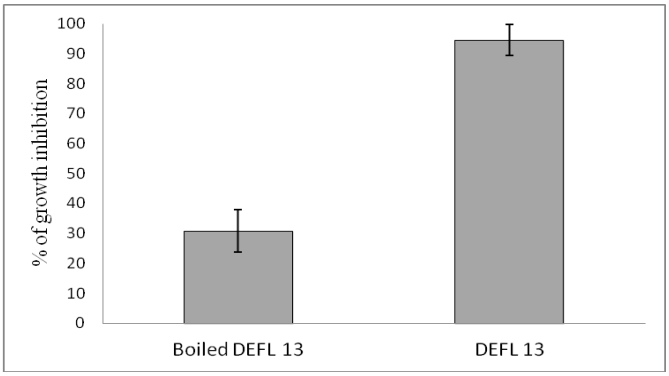


**Figure 4.14 Temperature effect on the antifungal activity of DEFL 13**. The percentage of growth inhibition on *B. cinerea* conidia treated with 50 µg/ml boiled (90°C for 10 min) DEFL 13 compared to untreated peptide.

### *4.3.5* Activity against fungal hyphae and protoplasts of *B. cinerea*

The ability of DEFL 13 to inhibit actively growing *B. cinerea* mycelium was also tested and compared to the inhibitory effect on conidia germination. This was evaluated *in vitro* both by microscopy observation and spectrophotometric readings. The *B. cinerea*

conidia were incubated overnight in half PDB before adding 50 µg/ml of DEFL 13. After 2 h the treated fungal hyphae showed morphological differences compared to untreated fungi since vacuolation appeared on the treated mycelia. (Figure 4.15). The percentage of growth inhibition after 48 h was calculated to be 81.5% (± 3.9), slightly less than the effect on the conidia germination reported above.

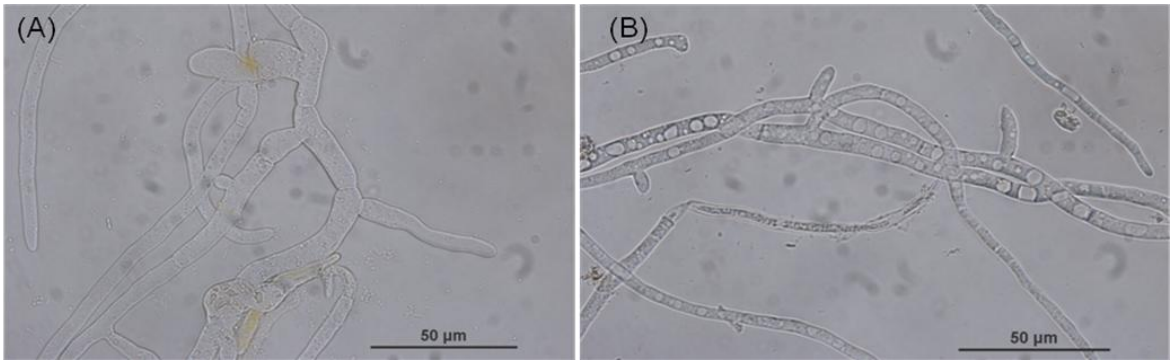


**Figure 4.15 Effect of DEFL 13 on actively growing *B. cinerea*.** Overnight germinated conidia were treated with (A) protein buffer and (B) 50 µg/ml of DEFL 13 and were observed at the optical microscope after 2 h of incubation. Scale bar= 50 µm

Fungal hyphae are surrounded by a cell wall that antimicrobial peptides must cross before reaching the plasma membrane. The effect of cell wall on the antifungal activity of DEFL 13 was investigated by incubating *B. cinerea* protoplasts with 50 µg/ml of recombinant peptide. After 24 h of treatment, the growth of protoplasts was inhibited of about 80%, compared to untreated protoplast culture (data not shown), indicating that cell wall is not crucial for antimicrobial activity of DEFL 13.

### 4.3.6 Membrane permeabilization and localization of DEFL 13

The effect of DEFL 13 on the fungal membrane was assayed, observing the uptake of the fluorescent dye SYTOX green within the treated fungal cells. DEFL 13 clearly induced SYTOX green uptake in *B. cinerea* hyphae: here, after 2 h of protein incubation, a high degree of fluorescence was detected (Figure 4.16). Incubation of fungal hyphae with protein buffer and SYTOX green did not show fluorescence uptake (data not shown).

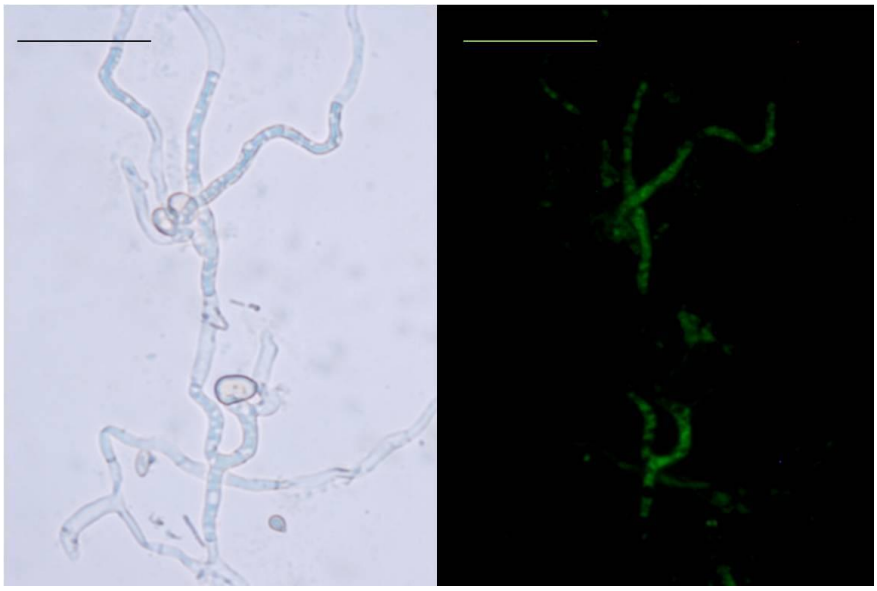

**Figure 4.16 SYTOX green uptake into DEFL 13 treated *B. cinerea*.** *B. cinerea* germinated conidia were incubated with 50 µg/ml of DEFL 13 and 1µM of SYTOX green and visualized by fluorescence microscopy after 2 h. The results of membrane permeabilization are representative of one triplicate experiment Scale bar= 50µm.

The DEFL 13 localization on treated fungal hyphae was addressed. The peptide was labeled with FITC and labeled protein was localized on *B. cinerea* hyphae by fluorescence microscopy. As labeling could possibly have a negative effect on the activity of DEFL 13, the antimicrobial activity of FITC-labeled DEFL 13 was tested against *B. cinerea*, showing to be the same than the one displayed by unlabelled protein form (data not shown). *B. cinerea* hyphae were treated with 50 µg/ml of FITC-labeled DEFL 13 for 1 h and the localization was monitored by fluorescence microscopy. As shown in Figure 4.17 FITC-labeled DEFL 13 appears mainly localized in the intracellular environment of *B. cinerea* treated hyphae.

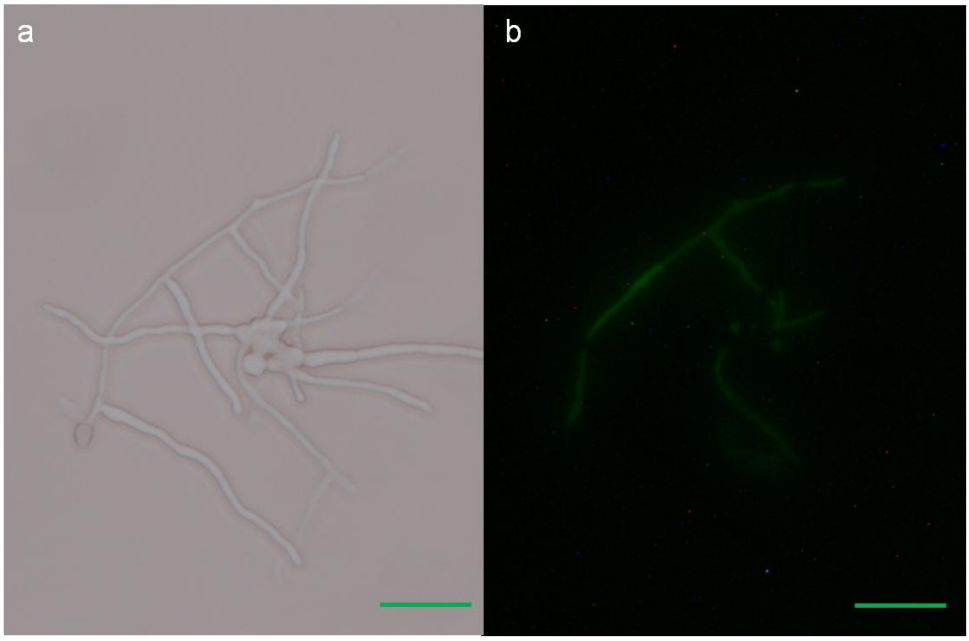


**Figure 4.17 Localization of FITC-labeled DEFL 13 *B. cinerea*.** Fungal hyphae of B. cinerea grown overnight in half PDB were treated with 50 μg/ml of FITC-labeled DEFL and after 1 h of incubation, the labeled peptide was detected by fluorescence microscopy. Bright field image (a) and fluorescence microscopy image (b). Scale bar = 50 μm

### 4.3.7 Activity of DEFL 13 on *B. cinerea* signaling mutants

It is reported that some plant defensins display their antimicrobial activity through activation of different intracellular mechanism, such ROS production, $Ca^{2+}$ influx alteration or interferation with cell cycle. Considering that DEFL 13 enters to the *B. cinerea* cells we decided to perform a screening on signaling mutants of *B. cinerea* in order to investigate a possible involvement of intracellular signaling cascades in DEFL 13 mechanism of action. The collection of mutants tested in this screening was generated by the group of Prof. Paul Tudzynski (University of Muenster, Germany). The mutants are knock-out mutants where the deletion of each target gene was performed by replacement vector carrying the hygromycin resistance cassette. The mutant collection includes mutants defective in cAMP, calcium and ROS signaling, sensore kinases and G-proteins. About 30 % of tested mutants (reported in the Table 4.7) showed a less sensitivity to DEFL 13 action. Decrease in sensitivity was considered significant when reached values < 60% .

| mutated gene | gene function |
|---|---|
| Bc1g_14021 | Bc- and Ss-specific ??? |
| Bc1g_02686 | Regulator of photolyases |
| Bc1g_11672 | Microsomal signal peptidase 12kD subunit |
| Δbtp1 | Transmembrane protein 1 (BTP1) [7-TM] |
| Δbcgpr1 | G protein-coupled receptor 1 |
| Δbcgpr3 | G protein-coupled receptor 3 |
| Δbcg1 | Gα subunit 1 (BCG1) |
| Δbcg2 | Gα subunit 2 (BCG2) |
| Δbcg3 | Gα subunit 3 (BCG3) |
| Δbcgb1 | Gβ subunit 1 (BcGB1) |
| Δbcgg1 | Gγ subunit 1 (BcGG1) |
| Δbac | Adenylatcyclase BAC |
| Δbcatf1 | ATF1 transcription factor |
| Δbap1 | AP1-like transcription factor |
| Δbcras2 | RAS-type GTPase BcRAS2 |
| Δbccdc42 | Rho-type GTPase BcCDC42 |
| Δbcbem1 | Scaffold protein |
| Δbcfar1 | Scaffold protein |

**Table 4.7 Signaling *B. cinerea* mutants with decreased susceptibility to DEFL 13 with respect to the wild type fungus.** DEFL 13 displayed a growth inhibition < than 60% against the reported mutants (three technical replicates).

The weaker antimicrobial activity were confirmed only for Bc1g_11672 (Microsomal signal peptidase 12kD subunit), Δbcgpr3 (G protein-coupled receptor 3), Δbccdc42 (Rho-type GTPase BcCDC42) and Δbcbem1 (scaffold protein), repeating the test in independent assays.

### 4.3.8 Polyclonal antibody against DEFL 13

The DGRCCKDHPKLGHCVP synthetic peptide (corresponding to DEFL 13 amino acid position 4 - 18) was used to immunize two rabbits and produce anti-DEFL 13 polyclonal antibody. The peptide was designed considering the prediction of antigenic determinants in the DEFL 13 primary sequence and the hydrophobicity of these regions. After Western blot titration, serum from rabbit 1 resulted more concentrated and specific than serum from rabbit 2 and it was selected for CNBr-sepharose affinity purification. A dilution 1:100 of purified antibody from serum of rabbit 1 (Figure 4.18) was used for Western blot analysis.

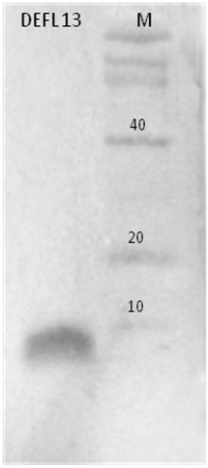


**Figure 4.18 Western blot assay of purified DEFL 13.**

### 4.3.9 *DEFL* 13 mutagenesis

Previous structure-function studies of cysteine-rich antimicrobial peptides from different organisms identified a conserved three-dimensional motif with a consensus sequence GXC($X_{3-9}$)C named γ-core motif (Yount NY *et al.* 2004). As above reported, DEFL 13 displays this motif, with the sequence of GLCKKLSSGRHVC and with a net positive charge (+3). Mutations in the primary sequence of γ-core motif altering the peptide cationicity and hydrophobicity were previously reported to strongly affect the antimicrobial function of plant defensins (Sagaram US *et al.* 2011). Site-directed mutagenesis of DEFL 13 was performed in order to investigate on the role of putative key residues on the DEFL 13 antifungal action. The mutations W30A, L42S, S48F, S48K and R50Q, mapping in the γ-core (L42S, S48F, S48K and R50Q) or in putative crucial sites for DEFL 13 structure (W30A) were generated (Table 4.8 and Figure 4.19)

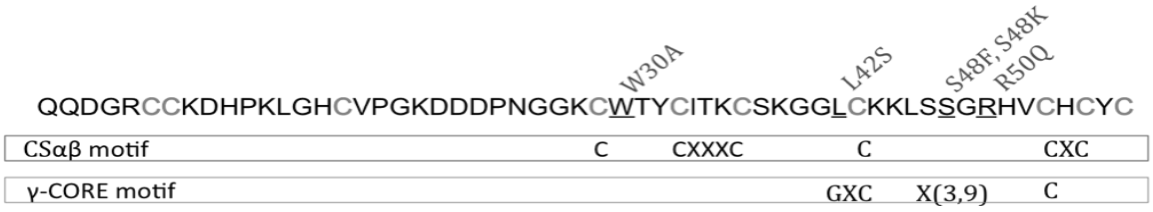


**Figure 4.19 Primary sequence of DEFL 13 and site-specific mutation.** The mutated amino acids are underlined and the substitutions are reported over them. CSαβ and γ core motifs are reported.

| Mutant | γ-core motif | | Comment |
|---|---|---|---|
| | Positive residues | GRAVY INDEX | |
| **Wild type** | **+3** | **-0,085** | |
| **W30A** | | | Tryptophan was replaced with Alanine to evaluate the effect of an high hydrophobic and structurally important residue on the antifungal activity. |
| **L42S** | +3 | -0,43 | Leucine was replaced with Serine to decrease the hydrophobicity in the γ-core motif. |
| **S48F** | +3 | 0,192 | Serine was replaced with Phenylalanine to increase the hydrophobicity in the γ-core motif. |
| **S48K** | +4 | -0,323 | Serine was replaced with Lysine to increase the positive charge of γ-core motif. |
| **R50Q** | +2 | -0,008 | Arginine was replaced with Glutamine to decraese the positive charge of γ-core motif. |

**Table 4.8 List of DEFL 13 mutants**. The variation of γ-core motif parameters and the comment are reported for each mutant. For the γ-core motif, the number of positive residues and the GRAVY* were reported for each mutation as calculated by Protparam (http://web.expasy.org/protparam). *GRAVY (grand average hydrophaticity index): positive GRAVY (hydrophobic), negative GRAVY (hydrophilic) (Kyte and Doolittle, 1982)

All mutants were expressed in the soluble fraction of *E. coli* SHuffle strain and purified to homogeneity (Figure 4.20 a) following the same protocol used for wild type DEFL 13 and yielding similar protein quantity. Protein integrity and identity were assayed by Western Blot (Figure 4.20 b).

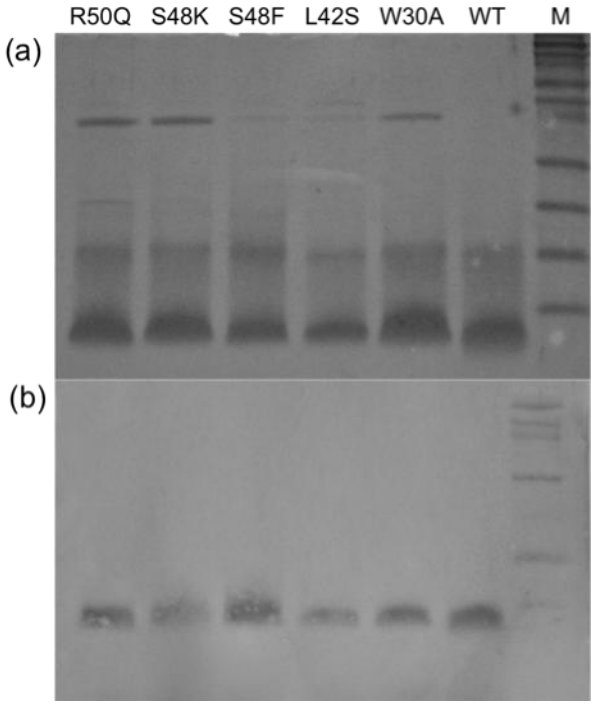


**Figure 4.20. (a) SDS-PAGE gel and (b) Western blot analyses of purified DEFL 13 and mutants.**

The purified W30A, L42S, S48F, S48K and R50Q mutants were able to induce membrane permeabilization in treated fungal hypahe of *B. cinerea* (Figure 4.21). Despite this test can not be considered a quantitative assay, a visual analysis showed that the tested DEFL 13 mutants displayed a different level of fluorescence uptake. In particular, the mutants S48K caused higher permeabilization in *B. cinerea* hyphae and the mutant L42S induced weaker membrane destabilization in treated mycelium.

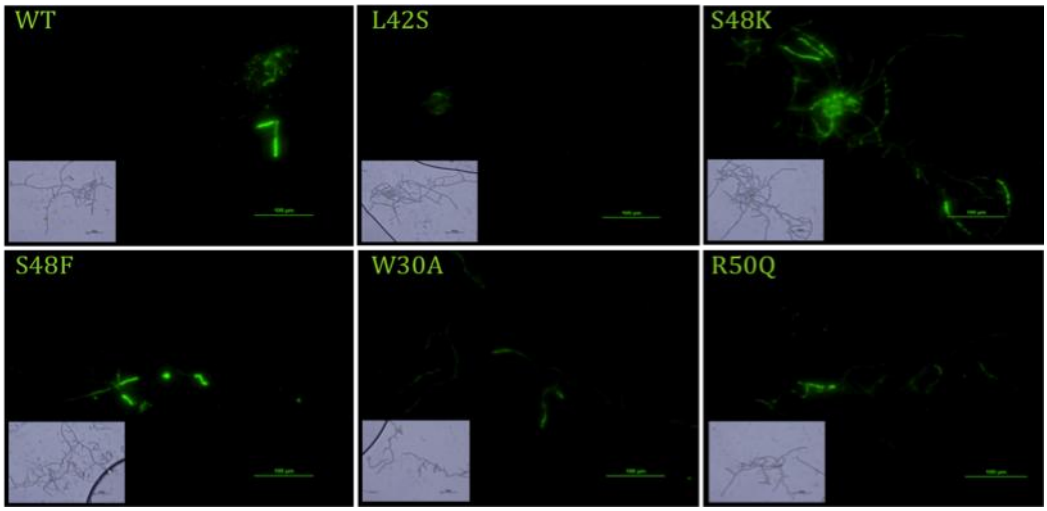


**Figure 4.21 SYTOX green uptake into *B. cinerea* treated with DEFL 13 and mutants (L42S, S48K, S48F, W30A, R50Q).** *B. cinerea* germinated conidia were incubated with 50 µg/ml of DEFL 13 (WT), L42S, S48K, S48F, W30A or R50Q and 1µM of SYTOX green and visualized by fluorescence microscopy after 2 h. In the small box the correspondent bright field images are reported. Scale bar= 50µm.

# 5 DISCUSSION

## 5.1 *DEFL* gene family in peach (*Prunus persica*) and grapevine (*Vitis vinifera*)

In different plant species DEFL peptides were recognized to be encoded by large multigene families: 317 and 92 *DEFL* genes have been identified in the *Arabidopsis thaliana* and *Oryza sativa* genomes respectively, whereas 369 *DEFL* EST sequences have been recognized in *Medicago truncatula* (Graham MA et al. 2004; Silverstein KA et al. 2005; Silverstein KA et al. 2007). The recent publication of *Prunus persica* (released by the International Peach Genome Initiative, IPGI, at the Genome Database for Rosaceae_http://www.rosaceae.org/peach/genom) and *Vitis vinifera* (Velasco R *et al.* 2007) genomes allowed investigation of the *DEFL* gene family in woody plant species. A BLAST search against the *P. persica* genome predicted peptide database, using PpDFN1 as query (the first plant defensin identified in peach, Wisniewski ME *et al*. 2003), identified other seven sequences encoding DEFLs. A more elaborated and extensive screening of the peach genome, using suitable matrices such as HMM (Hidden Markov Model), could probably reveal a higher number of *DEFL* genes also for this plant species. This was performed for grape (*V. vinifera*) where the use of successive iterations of HMM and BLAST searches resulted in the identification of 79 *DEFL* grapevine sequences followed by the full annotation of 46 *DEFL* genes (Giacomelli L *et al.* paper submitted).

In peach, the seven predicted DEFL peptides show high similarity with the previously reported PpDFN1. All of these display 8 cysteine residues, the typical CSαβ and γ core motifs. In grapevine, the majority of DEFL peptides display the typical defensin signatures: the signal peptide at the N-terminal, the CSαβ motif and the γ core motifs and contain 6, 8, or 10 cysteine residues in the mature protein sequence.

The high number of *DEFL* genes and the low identity in their primary sequences suggest that divergent selection events occurred following duplication and possibly providing new functions for these peptides. It has been indicated that the hypothesized evolution events leading to the *DEFL* gene family differentiation is striking similar to

those reported for the *NBS* (nucleotide binding site) and *LRR* (leucine rich-peptide) families of R-genes, both found as single gene and cluster throughout plant genomes (Graham MA *et al.* 2008). These similarities are compatible with an involvement of *DEFLs* genes in defense against pathogens.

## 5.2 Defensin from peach (*Prunus persica*): PpDFN1

### 5.2.1 Gene expression, antimicrobial activity and membrane interaction of the peach (*Prunus persica*) defensin PpDFN1

It is commonly believed that DEFL peptides act as preformed plant defence components in particular tissues or stages, such as dormant tissues or mychorrized roots, where inducible defence responses decrease. In addition to undergo a seasonal winter regulation in peach bark tissues, *Ppdfn1* gene expression was also shown to increase in fruits at early ripening stages, suggesting a role for this gene in protecting the embryo before seed lignification (Wisniewski ME *et al.* 2003). Consistently, our data show that this gene is more expressed during S1 and S2 ripening stages, before the fruit pit hardening has completed. It is known that the incidence of brown rot, caused by *M. laxa* and *fructigena* in peach, strongly decreases for a short period during fruit ripening (Mari M *et al.* 2003), in correspondence to the pit hardening, when the level of *Ppdfn1* transcript decreases. Since we show that recombinant PpDFN1 is able to inhibit *M. laxa* germination *in vitro*, it will be necessary to quantify the endogenous level of PpDFN1 in ripening fruits, to exclude a role for this peptide in the fruit defence against Monilia.

Our data show that the *Ppdfn1* gene expression is much higher in flower than fruit and leaf. Several plant *DEFL* genes were shown to be specifically expressed in flowers (Tavares LS *et al.* 2008), such as NaD1, a defensin from *Nicotiana alata* (van der Weerden NL *et al.* 2010) and PhD1 from *Petunia hybrida* (Janssen BJC *et al.* 2003). These defensins, and other flower DEFLs, were shown to be capable of antifungal activity against a broad spectrum of pathogens. Nevertheless, the flower specific DEFLs LURE 1 and LURE 2 from *Torenia fournieri*, besides being antifungal peptides, were shown to act as pollen attractants during plant fertilization (Okuda S *et al.* 2009), supporting the hypothesis that DEFL peptides can play additional roles during plant growth and development. Further studies are needed to evaluate the biological significance of *Ppdfn1* expression in

flower.

In order to investigate the activity of PpDFN1, the recombinant mature form of this peptide was overexpressed in *E. coli* and purified to homogeneity. The combination of *E. coli* Origami strain and pET32 expression vector was considered an efficient way to produce soluble recombinant protein with a high level of purity.

The purified PpDFN1 did not display any antimicrobial activity against human and plant bacterial pathogens but was capable of antifungal activity against *M. laxa, P. expansum* and *B. cinerea* fungi. The efficiency of PpDFN1 antifungal action depends on the fungal species, as shown by the calculated IC50 of 1.1, 9.9 and 15.1 μg/ml for *P. expansum, M. laxa* and B. *cinerea* respectively. For the majority of defensin peptides, the molecular mechanisms of the specificity of action are still not clear. Previous studies indicated that membrane destabilization is a common effect caused by these peptides in target cells (Thevissen K *et al.* 1996, van der Werdeen NL *et al.* 2010), suggesting that membrane composition of target cells could be an important determinant for the defensin activity. On the other hand, for some plant defensins further mechanisms were shown to specifically play a role. As an example NaD1, capable of membrane permeabilization in *Neurospora crassa,* was shown to enter fungal cells and induce ROS (Reactive Oxygen Species) production. The involvement of fungal membrane destabilization in the PpDFN1 antifungal activity was shown by SYTOX green assay for all tested fungi. However a lower level of fluorescence uptake was shown for *P. expansum*, suggesting a weaker permeabilization. Considering that PpDFN1 showed the highest antifungal activity against *P. expansum*, these data point to the involvement of other mechanisms leading to the observed inhibition of this fungal species.

Lipid monolayer is a simple membrane model system, that can be conveniently used to study the first step of membrane interaction. This system was used in order to investigate the possible correlation between PpDFN1 specificity and lipid membrane composition. Using films composed by different lipids, we obtained a qualitative analysis of the binding of PpDFN1 to lipids, determining its dependence on membrane composition.

Previous studies showed that plant and insect defensins interact with target cell membranes through binding to glucosylceramides lipid component (Thevissen K *et al.* 2004). Here we showed that the addition of the neutral sphingolipid ceramide β-D-galactoside to egg-phosphatidylcholine (ePC) membrane films significantly promoted the PpDFN1 lipid interaction. This reinforces the hypothesis that the presence of sphingolipid

species in target cell membranes is crucial for defensin action, as already indicated for RsAFP2 and DmAMP1 (Thevissen K *et al.* 2004; Aerts AM *et al.* 2008). Besides being an important structural component of eukaryotic membranes, sphingolipids are also recognized as secondary messenger molecules regulating the equilibria between cell death and cell growth processes. Interaction of plant defensins with these specific lipids can possibly lead to activation of signaling cascades promoting fungal growth arrest (Thevissen K *et al.* 2006).

Nevertheless, when films were made with lipid extracted directly from fungi, PpDFN1 bound to monolayer with higher affinity, suggesting that additional lipid components of fungal membranes play a role in this interaction. These could be the net negative charges of the fungal lipid extract (as inferred by the Zeta-potential measurements -data not shown-), electrostatically driving the positively charged defensin on the membrane, or other lipid species present in fungal membranes. These components are likely involved in the PpDFN1 specificity, as shown by the strong correlation between IC50 values and the monolayer measurements. Further investigations will be necessary to reveal the nature of the membrane components playing a role in this interaction and possibly to elucidate the molecular mechanisms of PpDFN1 antifungal activity.

## 5.3 Grapevine DEFLs

### 5.3.1 Recombinant expression and antimicrobial activity of grapevine (*Vitis vinifera)* DEFLs.

The identified grapevine *DEFL*s (Giacomelli L *et al.* paper submitted) sharing a common cysteine pattern were classified in three main groups(1, 2 and 3) and the remaining *DEFL*s were collected in a fourth additional group. The encoded DEFLs belonging to group 3 show the cysteine pattern previously reported for defensins identified in other plant species and for VvAMP1 (the only DEFL from grapevine previously known). On the contrary, the grapevine DEFLs belonging to the group 1 and 2 show a different cysteine pattern with respect to the plant defensins characterized until now.

In order to test the antimicrobial activity of grapevine DEFLs, *DEFL* 1, 13, 22, 31 and 59 were selected, since they belong to different groups (1, 2 and 3) and display a different tissue specificity or *B. cinerea* inducibility. Recombinant expression of DEFL 1,

belonging to group 1, failed and for this reason no members of group 1 were tested for their antimicrobial activity. The other selected DEFLs were successfully expressed only as protein fused to thioredoxin (TRX) or maltose binding protein (MBP) in *Escherichia coli*. In general, the presence of fusion tags at the N-terminal of the protein facilitates the expression in *E. coli* of proteins with a predicted complex folding, such as defensins. Until now, only PDC1 a plant defensin from corn (Kant P *et al.* 2009) was expressed without fusion tags in the soluble fraction of *E. coli*, as biological active peptide.

Several plant defensins were reported to inhibit the growth of *B. cinerea* with different efficiency. For examples DmAMP2 (a defensin from *Dhalia meckii*), HsAFP1 (a defensin from *Heuchera sanguine*) and RsAFP2 (a defensin from *Raphanus sativus*) showed IC50 values of 12, 10 and 6 μg/m1 respectively (Osborn *et al.* 1995).

All tested recombinant grapevine DEFLs are capable of inhibiting *B. cinerea* conidia germination. The most active protein (DEFL 13) is encoded by the *DEFL 13* gene, which was highly induced upon *B. cinerea* infection. The reported gene expression pattern and the antimicrobial activity *in vitro* suggest a defense role for DEFL 13 *in planta*.

The antifungal activity of the other tested DEFLs (22, 31 and 59) should be tested against a broader range of pathogens, in order to determine whether their weak effect against *B. cinerea* reflects a different biological role *in planta*. Since DEFL 59 and its more active partner DEFL 13 are both inflorescence specific, a different target or function would also justify their specific concomitant expression.

The loss of antibotrytis activity that follows the reduction and alkylation of DEFLs 13, 22, 31 and 59 indicates that, for these peptides, the disulphide bridges are necessary for the activity and their tertiary structure is crucial for antimicrobial activity. Similar results were obtained for NaD1 (a defensin from *Nicotiana alata*), where the disruption of its disulphide bonds resulted in the loss of antifungal activity (van der Weerden NL *et al.* 2008). On the other hand, oxidized species of human defensins 3 displayed the same antifungal potency (Wu Z et al. 2003) as the reduced one, indicating a dispensable role of corrected disulphide bridges for this peptide. None of the tested DEFLs display a morphogenetic action on the treated fungal mycelium. Indeed, in addition to the growth inhibitory activity, some defensin peptides (such as the Rs-AFP2 and the Hs-AFP1) are capable of hyphae swelling and hyperbranching on fungal target (Osborn *et al.* 1995). It was reported that the capacity to induce morphological effect on target fungi is not a specific characteristic of the protein but depends on the fungal target. The molecular mechanisms regulating the morphogenic action are still unknown.

### 5.3.2 DEFL 13

DEFL 13 has been selected for further analyses among the four above reported grapevine DEFLs for the following reasons:

(a) the strongest antimicrobial activity against *B. cinerea,*as indicated by the reported IC 50 values

*B. cinerea*, the grey mold fungus, infects more than 200 plant species and it is one of the most important grape pathogen. Plant diseases caused by *B. cinerea* are mainly characterized by rapid maceration of the plant tissue and massive production of conidia that can further distributed by wind, rain or insects (van Kan 2006). The inhibition of conidia germination is a crucial step for controlling and preventing the infection of the host plant and the discovery of antimicrobial peptides with a strong ability to inhibit the conidia germination is highly interesting for the plant protection.

(b) the original cysteine pattern in the primary sequence

DEFL 13 shows an interesting cysteine pattern in the primary sequence ($CCX_8CX_{12-13}CX_3CX_3CX_5CX_{8-9}CXCXC$) with ten cysteine residues all engaged in disulphide bridges as shown by the Ellman's test. PhD1, a defensin from *Petunia hybrida*, also displays 10 cysteine residues in the primary sequence but with a different arrangement (Janssen BJ *et al.* 2003).

#### 5.3.2.1 DEFL 13 purification

In the past several defensins were purified directly from the tissue where they resulted mainly expressed, for examples the defensin from *Phaseolus vulgaris* was directly purified from purple beans with a high yield (43 mg of purified defensin for 500 g of beans) (Wu X *et al.* 2011). However, not all defensins are necessarily present in high quantity and not always the protein purification from tissues, were the defensins are largely expressed, is easy to obtain (for example mature seeds of fruit where purification processes are difficult, due to lignification and oil content). In addition, different plant defensins are often expressed in the same tissue and the purification of a specific peptide is very difficult to obtain, due to the similar biochemical features shared by these peptides.

*DEFL 13* gene is highly expressed in inflorescence but the presence of other *DEFL* transcripts (such as *DEFL* 1, 2 and 59) makes DEFL 13 extraction from this tissue not suitable.

The expression of recombinant forms of proteins in heterologous systems is a direct and fairly simple way to overcome these problems. The production of plant defensins in heterologous system has widely been performed, in particular using *E. coli* (Figure 5.1).

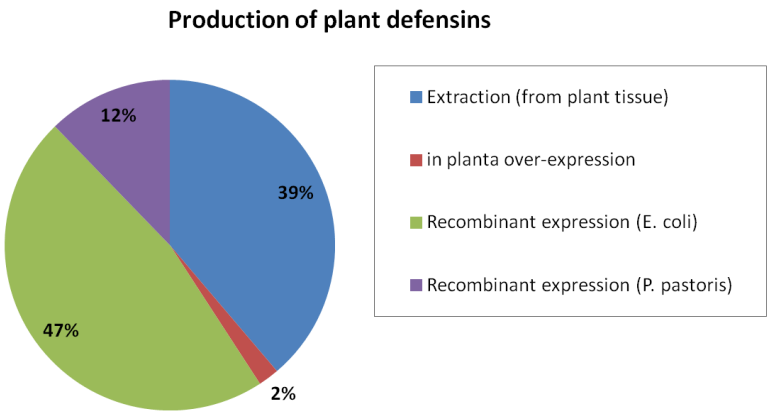


**Figure 5.1 Representation of the different strategies used for plant defensins production/isolation**. The percentages were determinated evaluating the production of 49 plant defensins.

It is known that lack of expression of eukaryotic proteins in prokaryotic organism is often due to the complexity of eukaryotic proteins respect to prokaryotic ones. Despite the small size and the simple structure of defensin proteins, the presence of several disulphide bridges, necessary to the protein stability, may impair the expression yield in *E. coli*. For this reason, protein expression in yeast were performed for several plant defensins, giving higher yields. However our attempts to produce DEFL 13 as recombinant protein in *P. pastoris* failed, indicating that folding process is not the only cause of low protein yield.

On the other hand the use of a different *E. coli* strain, specialized in disulphide bridge production, allowed significant improvement in DEFL 13 yield.

Furthermore for DEFL 13 and in general for the plant defensins tested in this PhD work, the choice of the expression vector has been crucial for the protein production. Tested DEFLs were successfully expressed when fused to TRX or MBP proteins and not when produced only with HIS-tag, consistently to the majority of plant defensins reported until now. Indeed, the presence of protein fusion partners can help to keep protein soluble during folding and to protect them from protein degradation by bacterial protease.

During protein purification it was observed a high leakage of proteins: the yield in

MBP-6xHis-DEFL 13 in *E. coli* lysate suspension was calculated to be about 20 times higher than the final yield in purified DEFL 13. High protein losses were associated with the steps of protein concentration and dialysis, suggesting that the high positive charge of DEFL 13 could be responsible for unspecific binding with membranes. A slight improvement has been achieved by performing protein chromatography in columns connected in series, avoiding buffer change and concentration step.

#### 5.3.2.2 Antimicrobial activity of DEFL 13

The antimicrobial action of DEFL 13 has been tested against different fungal pathogens and two bacteria attacking several plant crops. DEFL 13 did not display antimicrobial activity against the tested bacterial plant pathogens, consistently with the majority of plant defensins so far characterized. The concentration of DEFL 13 able to inhibit more than 90% of *B. cinerea* conidia germination had a weak effect on the other tested fungi (less than the 50%), with the exception of *A. niger* (62% values of fungal inhibition). This difference in antifungal potency is quite unusual among plant DEFLs, which normally display a broad range of antimicrobial activity against fungi. For examples Ah-AMP1, Ct-AMP1, Dm-AMP1, Hs-AFp1 and Rs-AFP2 showed a similar strong antifungal activity against *B. cinerea*, *Cladosporium sphaerospermum*, *Fusarium culmorum*, *Leptosphaeria maculans*, *Penicillium digitatum* and *Verticilium albo-atrum*. Also PpDFN1 (as reported above in this thesis) is highly active against all three tested fungi (*M. laxa*, *P. expansum* and *B. cinerea*). The molecular bases of DEFL 13 specificity are currently ignored. Possibly, a specific receptor in the cell membrane or a specific intracellular target in *B. cinerea* cytoplasm could be involved.

Cation sensitivity has been widely described for many basic antimicrobial peptides, which act via electrostatic interactions. Several works reported about the antagonist effect of cations on the antimicrobial activity of plant defensins (Terras FRG *et al.* 1992). It is commonly accepted that this reduction of activity is caused by an antagonist effect on the interaction of peptides with negative charged fungal membranes. De Samblanx and co-workers (De Samblax GW *et al*. 1997) suggested a model to explain this effect, where both ionic and non-ionic stereospecific interactions are involved in defensin action. The ionic components of the interaction are strongly affected by the ionic strength of the medium, instead the non ionic ones are cation-resistant, suggesting a putative receptor interaction. Furthermore, Thevissen and co-workers (Thevissen K *et al.* 1999) reported about the

dependence of membrane permeabilization on the cation composition of the medium, suggesting two different mechanisms of action: (i) a binding-site-mediated membrane insertion, not highly influenced by the presence of cations, and (ii) a binding-site-independent membrane insertion that is totally affected by ionic strength of the medium and involves only electrostatic interactions. The antimicrobial activity of DEFL 13 results strongly dependent on the ionic strength of the medium, in particular when divalent cations are added. The antifungal activity is reduced proportionally to the increase of cation concentration, with a complete abolishment of DEFL 13 activity at 5 mM of $MgCl_2$. Consistently with previous reported hypothesis, the high dependence of DEFL 13 antifungal activity on the cation composition of the medium suggests that the interaction between DEFL 13 and fungal membrane is mainly caused by electrostatic interaction with negative charged structures of fungal membranes. For this reason, the reported specificity of action for DEFL 13 against *B. cinerea* could be associated with an intracellular target rather than a specific receptor on the fungal membrane. However, additional experiments are necessary to support this hypothesis.

A significant variation in DEFL 13 antifungal activity has been also observed using different commercial PDB medium with different ionic composition. All together these data indicate that the antifungal potency of defensins in the presence of cations is important in order to evaluate the contribution of DEFL 13 in plant defense against pathogens.

DEFL 13 displays a strong antifungal activity not only towards germinating conidia but also against the mycelium of *B. cinerea*, determining a significantly reduction of fungal biomass. Microscope observations reveal enlargement of vacuoles in fungal treated hyphae, indicating that vacuolation could be involved in antimicrobial activity of DEFL 13. It was reported that toxic compounds produced by the antagonist action of *Alternaria alternata* in *Plasmopara viticola* cause drastic changes in fungal cell structure, such as abnormal vacuolation (Musetti R *et al.* 2006). The presence of enlarged vacuoles in fungal mycelium was reported to be a typical hallmark of programmed cell death by incompatibility (Pinan-Lucarrè B *et al.* 2005) and as effect of the presence of antagonist and/or toxic metabolites (Askary H *et al.* 1997). The tomato saponin α-tomatine induces cell death of *Fusarium oxysporum* through a programmed cell death together with a rapid generation of reactive oxygen species (ROS) in treated cells (Ito S *et al.* 2007). Among plant defensins, RsAFP2 and NaD1 induce ROS production in the human pathogen *Candida albicans* and in the filamentous fungi *Fusarium oxysporium* respectively (Aerts AM *et al.* 2007; van der Weerden *et al*. 2009).

DEFL 13 shows activity against *B. cinerea* protoplasts quantified as a percentage of growth inhibition slightly lower than the one shown against mycelium. In DEFL 13 activity, the cell wall does not appear a crucial factor for its antifungal function, in contrast with NaD1 that drastically reduced its activity against *F. oxysporum* depleted to the cell wall (van der Weerden et al. 2010). Our results suggest a direct interaction between peptide and fungal membrane, not influenced by cell wall components.

DEFL 13 is capable to induce strong membrane permeabilization in *B. cinerea* hyphae. Several defensins were also able to destabilize membranes (Thevissen K *et al.* 1999), supporting the hypothesis that the membrane permeabilization is a common step for plant defensins antimicrobial activity. Further knowledge on the DEFL 13 antibotrytis action are necessary to identify the specific mechanism of action leading to membrane permeabilization.

The interaction between fungi and FITC-labeled DEFL 13 was shown. After 1 h DEFL 13 already seems internalized in *B. cinerea* hyphae. Despite the membrane destabilization appears a common step for AMPs action, only few defensins were shown to be capable of entering the fungal cells. Similarly to DEFL 13, also PsD1 (a defensin from pea) and NaD1 localized inside the cells of sensitive fungi (Lobo DS *et al*. 2007; van der Weerden NL *et al.* 2008). For these two plant defensins additional mechanisms further than membrane destabilization contribute to the fungal death. Interaction with cyclin F and consequent affection of normal progression of cell cycle were necessary for PsD1 action, whereas ROS production was reported to occur in NaD1 treated fungi. It is possible that DEFL 13, upon internalization in *B. cinerea* cells, activates additional mechanisms responsible for fungal death.

In order to identify a possible intracellular target in fungal cells, a library of *B. cinerea* signaling mutant has been screened. The screening of signaling *B. cinerea* mutants revealed that intracellular signaling cascades could be involved in the antimicrobial activity of DEFL 13 against *B. cinerea*. The mutants that were characterized by increased DEFL 13 tolerance as compared to wild type are depleted in genes encoding proteins with pleiotropic effects on the cell metabolism. For example, a mutant that is less susceptible to the peptide is depleted of the gene cdc42, encoding for a rho-type GTPase involved in cell cycle regulation, suggesting a possible effect of the peptide in cell cycle progression as previously reported by Lobo DS and co-workers for PsD1 (Lobo DS *et al*. 2007). Furthermore, the higher resistance to DEFL 13 action associated with the mutant Δbcgpr3 (depleted to the gene encoding for a G protein-coupled receptor) could suggest a possible

contribute for this trans membrane receptor in antimicrobial peptides sensing. Consistently human α defensins were reported to interact with the G protein-coupled receptors (Yang D *et al.* 2000).

The intracellular localization of DEFL 13 in treated *B. cinerea* cells and the different DEFL 13 antifungal activity against mutants affected in important cell regulation pathways could suggest that intracellular mechanisms are involved in DEFL 13 action.

Site-direct mutagenesis of the γ-core motif was performed on DEFL 13 sequence. The γ-core motif (with a consensus sequence $GXC(X_{3-9})C$) is structurally composed by two anti-parallel β strands with an interposed loop that displays a net cationic charge. This motif is conserved among disulphide-containing antimicrobial peptides which target, interact, permeabilize, depolarize, activate receptors or interact with biomembranes. Previous works reported about the importance of γ-core motif for the antimicrobial action of plant defensins. Mutational analysis of RsAFP2 revealed that the amino acid residues important for antifungal activity clustered in two adjacent sites: one of this is between β-strands 2 and 3, corresponding to the γ-core motif. Furthermore, studies about MsDef1 (a defensin from *Medicago truncatula*) indicate that the γ-core motif contains the major determinants for its antifungal activity.

Both positive charged and hydrophobic residues of γ-core motif have been singularly mutated in DEFL 13 in order to obtain indications about possible crucial residues involved in peptide activity against *B. cinerea*.

All tested DEFL 13 mutants induced SYOTX green fluorescence uptake by *B. cinerea* treated fungal hyphae suggesting that the selected residues are not crucial for membrane destabilization. Despite this test can not be considered a quantitative assay, the S48K mutation, determining an increase of net positive charge in the γ-core motif, shows higher level of fluorescence uptake, possibly associated with a stronger membrane permeabilization. This supports the hypothesis that electrostatic interactions are important for DEFL 13-membrane interaction, at least during the first step. On the other hand, the mutant L42S, displaying a decrease in hydrophobicity level, shows a weaker level of fluorescence uptake, suggesting that also hydrophobicity contributes to this interaction. Consistently, Sagaram *et al.* (Sagaram US *et al.* 2011) proposed that there is a correlation between net positive charge of the peptide and its antifungal activity but this could be affect by hydrobobic residues.

#### 5.3.2.3 A model for DEFL 13 antibotrytis action

Taken together data reported in this study provide several important indications on the function of DEFL 13 and allowed to draw a model on the possible mechanism of action of DEFL 13 (Figure 5.2). The model takes into consideration that DEFL 13 shows a fairly specific antifungal activity both against germinating conidia and actively growing mycelium of the fungal pathogen *B. cinerea*. Antifungal activity appears strongly inhibited by the presence of cations in the medium. DEFL 13 destabilizes and permeabilizes fungal membranes and enters fungal hyphae. Furthermore, the antibiotic action of DEFL 13 is displayed through activation of some signaling cascade components.

Based on this model, DEFL 13 is electrostatically attracted to the negative charged lipids of the fungal membrane. After this, two possibilities are shown:

(i) the peptide is internalized and activates some intracellular cascades causing membrane permabilization and fungal death

(ii) the peptide causes membrane permeabilization and subsequently it is internalized

Both the mechanisms take into account the involvement of intracellular cascades; these cause fungal death by a mechanism not yet identified, that could affect the cell cycle regulation. The intracellular mechanisms activated by DEFL 13 could be the basis of the DEFL 13 specificity. Further experiments should be performed to support the hypothesis that the molecular basis of DEFL 13 specificity are not associated with membrane interaction.

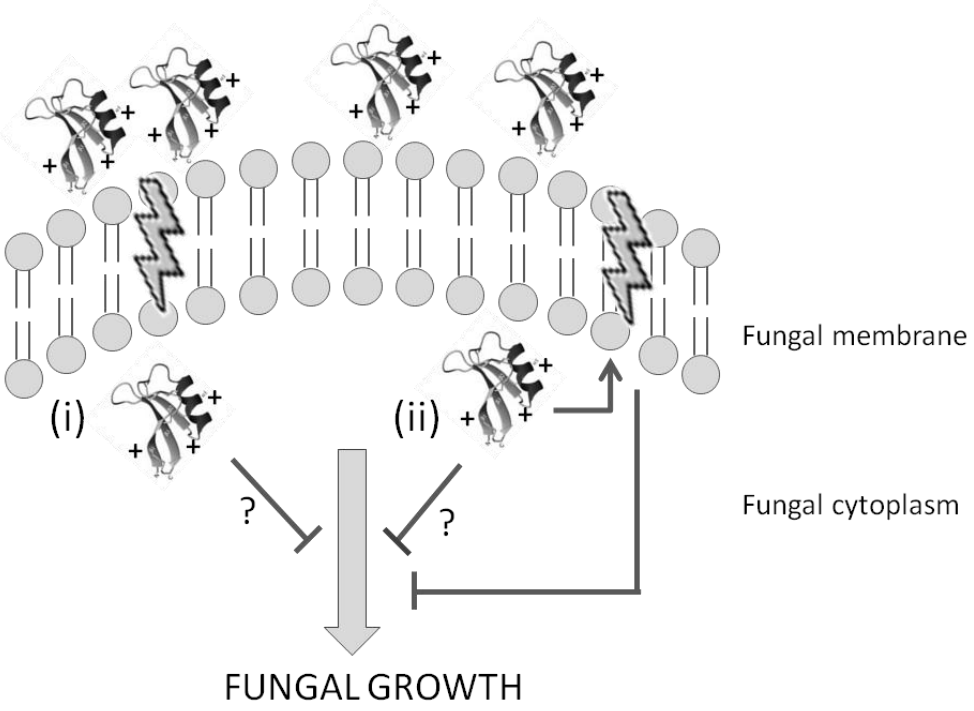


**Figure 5.2 Model of action of DEFL 13 on *B. cinerea* treated hyphae.** DEFL 13 is represented as NaD1 three-dimensional structures and lightning in the fungal membranes indicate membrane destabilization. The two possibilities are shown: (i) the peptide is internalized and activates some intracellular cascades causing membrane permabilization and fungal death. (ii) the peptide causes membrane permeabilization and subsequently it is internalized. The intracellular pathways activated by DEFL 13 and leading to the fungal death have not been yet characterized.

.

# 6 CONCLUSION REMARK

Several months of this PhD have been invested in protein expression and purification of DEFL peptides. Availability of these peptides is of a crucial importance for the characterization of their antimicrobial activity *in vitro* and for any possible exploitation of these compounds as antimicrobial agents. For this reason, the development of a simple and short protocol is currently under investigation.

The biological role of DEFL peptides *in planta* should be investigated also through quantification of the protein level, allowing a correlation between gene expression, antimicrobial activity *in vitro* and biological role. Furthermore, localization of DEFL peptides *in vivo* will be necessary to confirm a role for these peptides as defensins namely defense peptide acting extracellularly. Considering the strong cation sensitivity of DEFL 13, the antimicrobial activity should be also tested at plant physiological condition. A further depth evaluation of all these DEFLs properties will allow to confirm the defense role *in planta* of studied DEFLs.

# 7 BIBLIOGRAPHY


Aerts AM, François IEJA, Cammue BPA, Thevissen K, 2008. The mode of antifungal action of plant, insect, and human defensins. *Cell Mol Life Sci* 65, 2069-79.

Aerts AMa, François IEJA Els, Meert EMK and Li QT, 2007. The antifungal activity of RsAFP2, a plant defensin from *Raphanus sativus* , involves the induction of reactive oxygen species in *Candida albicans*. *J Mol Microbiol Biotechnol* 13, 243–247

An SH, Choi HW, Hwang IS, Hong JK,Hwang BK, 2008. A novel pepper membrane-located receptor-like protein gene CaMRP1 is required for disease susceptibility, methyl jasmonate insensitivity and salt tolerance. *Plant Mol Biol* 67, 519–33.

Askary H, Benhamou N, Brodeur J,1997. Ultrastructural and cytochemical investigations of the antagonistic effect of *Verticillium lecanii* on cucumber powdery mildew. *Phytopathology* 87, 359-368;

Berrow NS, Alderton D, Sainsbury S, Nettleship J, Assenberg R, Rahman N, Stuart DI, Owens RJ, 2007. A versatile ligation-independent cloning method suitable for high-throughput expression screening applications. *Nucleic Acids Res* 35(6):e45

Bonghi C, Rascio N, Ramina A, Casadoro G, 1992. Cellulase and polygalacturonase involvement in the abscission of leaf and fruit explants of peach. *Plant Mol Biol* 20, 839-848

Brogden KA, 2005. Antimicrobial peptides: pore formers or metabolic inhibitors in bacteria? *Nat Rev Microbiol* 3, 238-250

Carvalho AO and Gomes VM, 2009. Plant defensins-prospects for the biological functions and biotechnological properties. *Peptides* 30, 5, 1007-20

Chen GH, Hsu MP, Tan CH, Sung HY, Kuo CG, Fan MJ, Chen HM, Chen S and Chen CS, 2005. Cloning and characterization of a plant defensin VaD1 from azuki bean. *J*

*Agric Food Chem* 23, 53 4, 982-8

Cornet B, Bonmatin JM, Hetru C, Hoffmann JA, Ptak M, Vovelle F, 1995. Refined three-dimensional solution structure of insect defensin A. *Structure* 3, 435–48.

de Beer A and Vivier MA, 2008. Four plant defensins from an indigenous South African Brassicaceae species display divergent activities against two test pathogens despite high sequence similarity in the encoding genes. *BMC Plant Biol* 8, 8-75

de Medeiros LN, Angeli R, Sarzedas CG, Barreto-Bergter E, Valente AP, Kurtenbach E and Almeida FC, 2010. Backbone dynamics of the antifungal Psd1 pea defensin and its correlation with membrane interaction by NMR spectroscopy. *Biochim Biophys Acta*.1798(2):105-13.

de Paula VS, Razzera G, Barreto-Bergter E, Almeida FC and Valente AP, 2011. Portrayal of complex dynamic properties of sugarcane defensin 5 by NMR: multiple motions associated with membrane interaction. *Structure* 19(1):26-36.

de Samblanx GW, Goderis IJ, Thevissen K, Raemaekers R, Fant F, Borremans F, Acland DP, Osborn RW, Patel S and Broekaert WF, 1997. Mutational analysis of a plant defensin from radish (*Raphanus sativus L*.) reveals two adjacent sites important for antifungal activity. *J Biol Chem*.10, 272(2), 1171-9.

Ellman GL, 1958. A colorimetric method for determining low concentrations of mercaptans. *Arch Biochem Biophys* 74, 443-450

Fant F, Vranken W, Broekaert W and Borremans F, 1998. Determination of the three-dimensional solution structure of *Raphanus sativus* antifungal protein 1 by 1H NMR. *J Mol Biol* 29, 257-270.

Folch J , Lees M, Sloane Stanley GH, 1957. Simple method for the isolation and purification of total lipids from animal tissues. *The Journal Of Biological Chemistry* 226, 497-509.

Fossdal CG, Nagy NE, Sharma P,Lönneborg T, 2003. The putative gymnosperm plant defensin polypeptide (SPI1) accumulates after seed germination, is not readily released, and the SPI1 levels are reduced in *Pythium dimorphum*-infected spruce roots. *Plant Molecular Biology* 52, 291–302.

Giesbert S, Schumacher J, Segmueller N, Haeuser-Hahn I, Schreier P, Tudzynski P. Identification of pathogenesis associated genes by T-DNA-mediated insertional mutagenesis in *Botrytis cinerea*: a type 2A phosphoprotein phosphatase and a SPT3 transcription factor have significant impact on virulence. *MPMI* Accepted for publication.

Graham MA, Silverstein KA, Cannon SB, VandenBosch KA, 2004. Computational identification and characterization of novel genes from legumes. *Plant Physiol.* 135, 1179-97.

Graham MA, Silverstein KAT and VandenBosch, 2008. A Defensin-like Genes: genomic perspectives on a diverse superfamily in Plants. *The plant genome* S3-S9

Hammami R, Hamida JB, Vergoten G and Fliss I, 2009. PhytAMP: a database dedicated to antimicrobial plant peptides. *Nucleic Acid Res* 37, 963-968

Iriti M and Faoro F, 2007. Review of innate and specific immunity in plants and animals. *Mycopathologia* 164, 2:57-64.

Janssen BJC, Schirra HJ, Lay FT, Anderson MA,Craik DJ, 2003. Structure of *Petunia hybrida* Defensin 1, a novel plant defensin with five disulfide bonds. *Biochemistry* 42, 8214-22.

Jones JD and Dangl JL, 2006. The plant immune system. *Nature* 16, 323-9. Review.

Kant P, Liu WZ and Pauls KP, 2009. PDC1, a corn defensin peptide expressed in *Escherichia coli* and *Pichia pastoris* inhibits growth of *Fusarium graminearum*. *Peptides* 30, 1593-9.

Kanzaki H, Nirasawa S, Saitoh H, Ito M, Nishihara M, Terauchi R and Nakamura I, 2002. Overexpression of the wasabi defensin gene confers enhanced resistance to blast fungus ( *Magnaporthe grisea*) in transgenic rice. *Theor Appl Genet* 105, 809-814.

Klimpel A, Gronover CS, Williamson B, Stewart JA and Tudzynski P, 2002. The adenylate cyclase (BAC) in *Botrytis cinerea* is required for full pathogenicity. *Mol Plant Pathol* 6, 439-450

Kokkelink L, Minz A, Al-Masri M, Giesbert S, Barakat R, Sharon A and Tudzynski P, 2011. The small GTPase BcCdc42 affects nuclear division, germination and virulence of the gray mold fungus *Botrytis cinerea*. Fungal Genet Biol 48, 1012-9

Kyte J and Doolittle RF, 1982. A simple method for displaying the hydropathic character of a protein. *J Mol Biol* 5, 105-32

Larkin MA, Blackshields G, Brown NP, Chenna R, McGettigan PA, McWilliam H, Valentin F, Wallace IM, Wilm A, Lopez R, Thompson JD, Gibson TJ, Higgins DG, 2007. Clustal W and Clustal X version 2.0. *Bioinformatics* 23, 2947-2948

Lobo DS, Pereira IB, Fragel-Madeira L, Medeiros LN, Cabral LM, Faria J, Bellio M, Campos RC, Linden R, Kurtenbach E, 2007. Antifungal *Pisum sativum* Defensin 1 interacts with *Neurospora crassa* Cyclin F related to the cell cycle. *Biochemistry* 46, 987-96.

Manners JM, Penninckx IA, Vermaere K, Kazan K, Brown RL, Morgan A, Maclean DJ, Curtis MD, Cammue BP and Broekaert WF, 1998. The promoter of the plant defensin gene PDF1.2 from Arabidopsis is systemically activated by fungal pathogens and responds to methyl jasmonate but not to salicylic acid. *Plant Biol Mol* 38,6:1071-80

Mari M, Casalini L, Baraldi E, Bertolini P, Pratella GC, 2003. Susceptibilty of apricot and peach fruit to *Monilinia laxa* during phenological stages. *Postharvest Biology and Technology* 30, 105-109.

Mendez E, Moreno A, Colilla F, Pelaez F, Limas GG, Mendez R, Soriano F, Salinas M, de Haro C, 1990. Primary structure and inhibition of protein synthesis in eukaryotic cell-free system of a novel thionin, gamma-hordothionin, from barley endosperm. *Eur J Biochem* 12, 533-9

Meyer B, Houlné C, Pozueta-Romero' J, Schantz ML and Schantz R,1996. Fruit-specific expression of a defensin-type gene family in bell pepper. *Plant Physiol* 112, 615-22.

Mirouze M, Sels J, Richard O, Czernic P, Loubet S, Jacquier A, François I EJA, Cammue BPA, Lebrun M, Berthomieu P, Marquès L, 2006. A putative novel role for plant defensins: a defensin from the zinc hyper-accumulating plant, *Arabidopsis halleri*, confers zinc tolerance. *The Plant Journal* 47, 329–42

Musetti R, Polizzotto R, Vecchione A, Borselli S, Zulini L, D'Ambrosio M, Sanita` di Toppi L, Per tot I, 2007. Antifungal activity of diketopiperazines extracted from *Alternaria alternata* against *Plasmopara viticola*: An ultrastructural study. *Micron* 38, 643–650

Okuda S, Tsutsui H, Shiina K, Sprunck S, Takeuchi H, Yui R, Kasahara RD, Hamamura Y, Mizukami A, Susaki D, Kawano N, Sakakibara T, Namiki S, Itoh K, Otsuka K, Matsuzaki M, Nozaki H, Kuroiwa T, Nakano A, Kanaoka MN, Dresselhaus T, Sasaki N, Higashiyama T, 2009. Defensin like polypeptide LUREs are pollen tube attractants secreted from synergid cells. *Nature* 458, 357-61.

Oomen RJFJ, Séveno-Carpentier E, Ricodeau NN, Bournaud C, Conéjéro G, Paris N, Berthomieu P and Marquès L, 2011. Plant defensin AhPDF1.1 is not secreted in leaves but it accumulates in intracellular compartments. *New Phytologist* 192, 1:140-150

Osborn RW, De Samblanx GW, Thevissen K, Goderis I, Torrekens S, Van Leuven F, Attenborough S, Rees SB, Broekaert WF, 1995. Isolation and characterisation of plant defensins from seeds of Asteraceae, Fabaceae, Hippocastanaceae and Saxifragaceae. *FEBS Lett* 17, 257-62.

Penninckx IAMA, Eggermont K, Terras FRG, Thomma BPHJ, De Samblanx GW, Buchala A, Métraux JP, Manneqa JM, Broekaert WF, 1996. Pathogen-induced systemic activation of a plant defensin gene in Arabidopsis follows a salicylic acid-independent pathway. *The Plant Cell* 8, 2309-23.

Peranen J, Rikkonen M, Hyvonen M, Kaarlainen L, 1996. T7 vectors with a modified T7lac promoter for expression of protein in *Escherichia coli*. Analytical biochemistry 236:371-373

Pinan-Lucarré B, Balguerie A, Clavé C, 2005. Accelerated cell death in Podospora autophagy mutants. *Eukaryotic Cell* 4,1765-1774

Portieles R, Ayra1 C, Gonzalez E, Gallo A, Rodriguez R, Chaco O, Lopez Y, Rodriguez M, Castillo J, Pujol M, Enriquez G, Borroto C, Trujillo L, Thomma BPHJ, Borràs-Hidalgo O, 2010. NmDef02, a novel antimicrobial gene isolated from *Nicotiana megalosiphon* confers high-level pathogen resistance under greenhouse and field conditions. Plant Biotechnol J 6, 678-690

Rice P, Longden I, Bleasby A, 2000. EMBOSS: The European Molecular Biology Open Software Suite. *Trends in Genetics* 16, 276-277

Rolke Y, Liu S, Quidde T, WilliamsonB, Schouten A, Weltring KM, Siewers V, Tenberge KB, Tudzynski B and Tudzynski P, 2004.Functional analysis of H(2)O(2)-generating systems in *Botrytis cinerea*: the major Cu-Zn-superoxide dismutase (BCSOD1) contributes to virulence on French bean, whereas a glucose oxidase (BCGOD1) is dispensable. *Mol Plant Pathol* 1, 17-27

Sagaram US, Pandurangi R, Kaur J, Smith TJ and Shah DM, 2011. Structure-activity determinants in antifungal plant defensins MsDef1 and MtDef4 with different modes of action against Fusarium graminearum. PLoS One 13, 6(4):e18550.

Schaaper WM, Posthuma GA, Plasman HH, Sijtsma L, Fant F, Borremans FA, Thevissen K, Broekaert WF, Meloen RH and van Amerongen A. 2001. Synthetic peptides derived from the beta2-beta3 loop of *Raphanus sativus* antifungal protein 2 that mimic the active site. *J Pept Res* 57, 409-418.

Schulze Gronover C, Kasulke D, Tudzynski P and Tudzynski B, 2001.The role of G protein alpha subunits in the infection process of the gray mold fungus Botrytis cinerea. *Mol Plant Pathol* 11, 1293-1302

Schulze Gronover C., Schumacher, J., Hantsch, P., and Tudzynski, B, 2005. A novel seven-helix transmembrane protein BTP1 of *Botrytis cinerea* controls expression of GST-encoding genes, but is not essential for pathogenicity. *Mol. Plant Pathol*. 6, 243-256.

Schumacher, J., de Larrinoa IF and Tudzynski B, 2008. Calcineurin-responsive zinc finger transcription factor CRZ1 of Botrytis cinerea is required for growth, development and full virulence on bean plants. *Eukaryot cell*. 4, 584-601

Schumacher, J., Kokkelink L, Huesmann C, Jimenez-Teja D, Collado IG, Barakat R, P., Tudzynski P and Tudzynski B, 2008. The cAMP-dependent signaling pathway and its role in conidial germination, growth and virulence of the gray mold *Botrytis cinerea*. *Mol. Plant Microbe Interact*. 11, 1443-1459

Silverstein KA, Graham MA, Paape TD and VandenBosch KA, 2005. Genome organization of more than 300 defensin-like genes in Arabidopsis. *Plant Physiol* 138, 600-10.

Silverstein KA, Moskal WA Jr, Wu HC, Underwood BA, Graham MA, Town CD, VandenBosch KA, 2007. Small cysteine-rich peptides resembling antimicrobial peptides have been under-predicted in plants. *Plant J.* 51, 262-80.

Spelbrink RG, Dilmac N, Allen A, Smith TJ, Shah DM, Hockerman GH, 2004. Differential antifungal and calcium channel-blocking activity among structurally related plant defensins. *Plant Physiol* 135, 2055-67

Tavares LS, Santos MDO, Viccini LF, Moreira JS, Miller RNG, Franco OL, 2008. Biotechnological potential of antimicrobial peptides from flowers. *Peptides* 29, 1842-51

Temme N and Tudzynski P, 2009. Does *Botrytis cinerea* ignore H(2)O(2)-induced oxidative stress during infection? Characterization of botrytis activator protein 1.*Mol Plant Microbe interact* 8, 987-998

Terras FR, Eggermont K, Kovaleva V, Raikhel NV, Osborn RW, Kester A, Rees SB, Torrekens S, Van Leuven F and Vanderleyden J, 1995. Small cysteine-rich antifungal proteins from radish: their role in host defense. *Plant Cell* 7, 573-88

Terras FR, Schoofs HM, De Bolle MF, Van Leuven F, Rees SB, Vanderleyden J, Cammue BP and Broekaert WFJ, 1992. Analysis of two novel classes of plant antifungal proteins from radish (*Raphanus sativus L.*) seeds. *Biol Chem*. 5, 15301-9.

Terras FRG, Torrekens S, Leuvenb FV, Osborn RW", Vanderleyden J, Cammue BPA and Broekaert WF, 2005. A new family of basic cysteine-rich plant antifungal proteins from Brassicaceae species. *FEBS Letters* 316, 233-240

Thevissen K, Cammue BP, Lemaire K, Winderickx J, Dickson RC, Lester RL, Ferket KK, Van Even F, Parret AH and Broekaert WF, 2000. A gene encoding a sphingolipid biosynthesis enzyme determines the sensitivity of Saccharomyces cerevisiae to an antifungal plant defensin from dahlia (Dahlia merckii).*Proc Natl Acad Sci U S A.*15;97(17):9531-6.

Thevissen K, Ferket KK, François IE and Cammue BP, 2003. Interactions of antifungal plant defensins with fungal membrane components. *Peptides* 24(11):1705-12

Thevissen K, François IE, Winderickx J, Pannecouque C and Cammue BP, 2006. Ceramide involvement in apoptosis and apoptotic diseases. *Mini Rev Med Chem.* 6(6):699-

Thevissen K, Francois IE, Winderickx J, Pannecouque C, Cammue BP, 1996. Ceramide involvement in apoptose and apoptic diseases. *Mini Rev Med Chem* 6, 699-709.

Thevissen K, Ghazi A, De Samblanx GW, Brownlee C, Osborn RW, Broekaert WF, 1996. Fungal membrane responses induced by plant defensins and thionins. *J Biol Chem* 271, 15018-25.

Thevissen K, Osborn W, Acland DP and Broekaert WF, 1997. Specific, high affinity binding sites for an antifungal plant defensin on *Neurospora crassa* hyphae and microsomal membranes. *J Biol Chem*. 272(51):32176-81.

Thevissen K, Terras FR and Broekaert WF, 1999. Permeabilization of fungal membranes by plant defensins inhibits fungal growth. *Appl Environ Microbiol*. 65, 5451-8.

Thevissen K, Warnecke DC, François IEJA., Leipelt M, Heinz E, Ott C, Zähringer U, Thomma BPHJ, Ferket KKA, Cammue BPA, 2004. Defensins from insects and plants interact with fungal glucosylceramides. *J Biol Chem* 279, 3900-3905.

van der Weerden NL, Hancock RE, and Anderson MA, 2010. Permeabilization of fungal hyphae by the plant defensin NaD1 occurs through a cell wall-dependent process. *J Biol Chem* 26, 285 48:37513-20

van der Weerden NL, Hancock REW, Anderson MA, 2010. Permeabilization of fungal hyphae by the plant defensin NaD1 occurs through a cell wall-dependent process. J Biol Chem 285, 37513-20.

van der Weerden NL, Lay FT, Anderson MA, 2008. The plant defensin, NaD1, enters the cytoplasm of *Fusarium oxysporum* hyphae. *J Biol Chem* 283, 14445-14452.

van Kan JA, 2006. Licensed to kill: the lifestyle of a necrotrophic plant pathogen. *Trends Plant Sci* 11, 247-53. Review

Velasco R, Zharkikh A, Troggio M, Cartwright DA, Cestaro A, Pruss D, Pindo M, Fitzgerald LM, Vezzulli S, Reid J et al. 2007. A high quality draft consensus sequence of the genome of a heterozygous grapevine variety. *PLoS One* 2(12):e1326.

Wilmes M, Cammue BPA, Sahl HG and Thevissen K, 2011. Antibiotic activities of

host defense peptides: more to it than lipid bilayer perturbation. *Nat. Prod. Rep.* DOI:10.1039/c1np00022e

Wisniewski ME, Bassett CL, Artlip TS, Webb RP, Janisiewicz WJ, Norelli JL, Goldway M, Droby S, 2003. Characterization of a defensin in bark and fruit tissues of peach and antimicrobial activity of a recombinant defensin in the yeast, *Pichia pastoris*. *Physiologia plantarum* 119, 563-72.

Withmore L, Wallace BA, 2004. DICHROWEB, an online server for protein secondary structure analyses from circular dichroism spectroscopic data. *Nucleic Acids Res* 1, 668-673

Wu X, Sun J, Zhang G, Wang H, Ng TB, 2011. An antifungal defensin from *Phaseolus vulgaris* cv. 'Cloud Bean'. *Phyomedicine* 15, 104-9

Wu Z, Hoover DM, Yang D, Boulègue C, Santamaria F, Oppenheim JJ, Lubkowski J, Lu W,2003.Engineering disulfide bridges to dissect antimicrobial and chemotactic activities of human beta-defensin 3. *Proc Natl Acad Sci U S A.* 22, 8880-5.

Yang D, Biragyn A, Kwak LW, Oppenheim JJ, 2002. Mammalian defensins in immunity: more than just microbicidal. *Trends Immunol. 23*, 291–296

Yount NY,Yeaman MR, 2004. Multidimensional signatures in antimicrobial peptides. *PNAS* 101, 7363-8.